Precambrian Research 348 (2020) 105864

Contents lists available at ScienceDirect

Precambrian Research

journal homepage: www.elsevier.com/locate/precamres

Hydrothermal genesis of Nb mineralization in the giant Bayan Obo REE-Nb-Fe deposit (China): Implicated by petrography and geochemistry of Nb-bearing minerals

Shang Liu[a,*], Lin Ding[a,b], Hong-Rui Fan[c,d,e], Kui-Feng Yang[c,d,e], Yan-Wen Tang[f], Hai-Dong She[c,d], Mei-zhen Hao[g]

[a] School of Earth Sciences, Lanzhou University and Key Laboratory of Mineral Resources in Western China (Gansu Province), Lanzhou 730000, China
[b] Institute of Tibetan Plateau Research, Chinese Academy of Sciences, Beijing 100101, China
[c] Key Laboratory of Mineral Resources, Institute of Geology and Geophysics, Chinese Academy of Sciences, Beijing 100029, China
[d] College of Earth and Planetary Sciences, University of Chinese Academy of Sciences, Beijing 100049, China
[e] Innovation Academy for Earth Science, Chinese Academy of Sciences,Beijing 100029, China
[f] State Key Laboratory of Ore Deposit Geochemistry, Institute of Geochemistry, Chinese Academy of Sciences, Guiyang 550002, China
[g] Bayan Obo Iron Mine, Baotou Iron and Steel Group, Baotou 014080, China

ARTICLE INFO

Keywords:
Nb mineralization
Nb-bearing minerals
Hydrothermal
Bayan Obo REE-Nb-Fe deposit

ABSTRACT

The Bayan Obo REE-Nb-Fe deposit, which reserves the current largest REE resources globally, also hosts over 70% of China's Nb resources. Unlike many world-class carbonatite-related Nb deposits (e.g. Morro dos Seis Lagos and Araxá, Brazil) with igneous or secondary origin, Nb was mainly stored in Nb-bearing minerals (aeschynite, ilmenorutile, baotite, fergusonite etc.) of hydrothermal origin at Bayan Obo, supported by evidence from petrography, element and isotopic geochemistry. Although igneous fersmite and columbite were occasionally discovered in local carbonatite dykes, the Mesoproterozoic and Paleozoic hydrothermal metasomatism occurred in the ore-hosting dolomite, related to carbonatite intrusion and the closure of Paleo-Asian Ocean respectively, has played a more significant role during the ultimate Nb enrichment. REE, however, was significantly enriched during both the carbonatite-related magmatic and hydrothermal processes. Consequently, there was differentiated mineralization between REE and Nb in the carbonatite dykes and the ores. Niobium mineralization at Bayan Obo is rather limited in Mesoproterozoic carbonatite, whereas more extensive in the metasomatized ore-hosting dolomite, and generally postdating the REE mineralization at the same stage. According to mineral geochemistry, Bayan Obo aeschynite was classified into 3 groups: aeschynite-(Nd) with convex REE patterns (Group 1); aeschynite-(Ce) (Group 2) and nioboaeschynite (Group 3) with nearly flat REE patterns. Aeschynite (Group 1), ilmenorutile and fergusonite precipitated from Paleozoic hydrothermal fluids with advanced fractionation of Ce-rich REE minerals. The Mesoproterozoic hydrothermal Nb mineralization, represented by aeschynite (Group 3) and baotite, occurred postdating REE mineralization at same stage. Besides, fersmite and aeschynite (Group 2) precipitated from the Mesoproterozoic REE-unfractionated melt and hydrothermal fluids, respectively. All above Nb-bearing minerals exhibit extreme Nb-Ta fractionation as a primary geochemical characteristic of mantle-derived carbonatite. The forming age of the aeschynite megacrysts (Group 1) has not been accurately determined. However, the potential age was constrained to ~430 Ma or alternatively ~270–280 Ma subjected to subduction and granite activity, respectively. These aeschynite crystals inherited REEs from multiphase former REE mineralization, with an intermediate apparent Sm-Nd isochron age between the Mesoproterozoic and the Paleozoic REE mineralization events.

1. Introduction

Niobium is a critical element for steel and nuclear industries. Over 90% of the current Nb resources are stored and produced in Brazil and Canada (Mackay and Simandl, 2014; USGS, 2019). Globally, most Nb deposits are closely related to carbonatite, alkali granitoids, pegmatite and their weathered layers, among which carbonatite is the major host of high grade Nb ores (Simandl et al., 2018). The largest and second

* Corresponding author.
E-mail address: liushang@lzu.edu.cn (S. Liu).

https://doi.org/10.1016/j.precamres.2020.105864
Received 17 March 2020; Received in revised form 4 July 2020; Accepted 13 July 2020
Available online 18 July 2020
0301-9268/

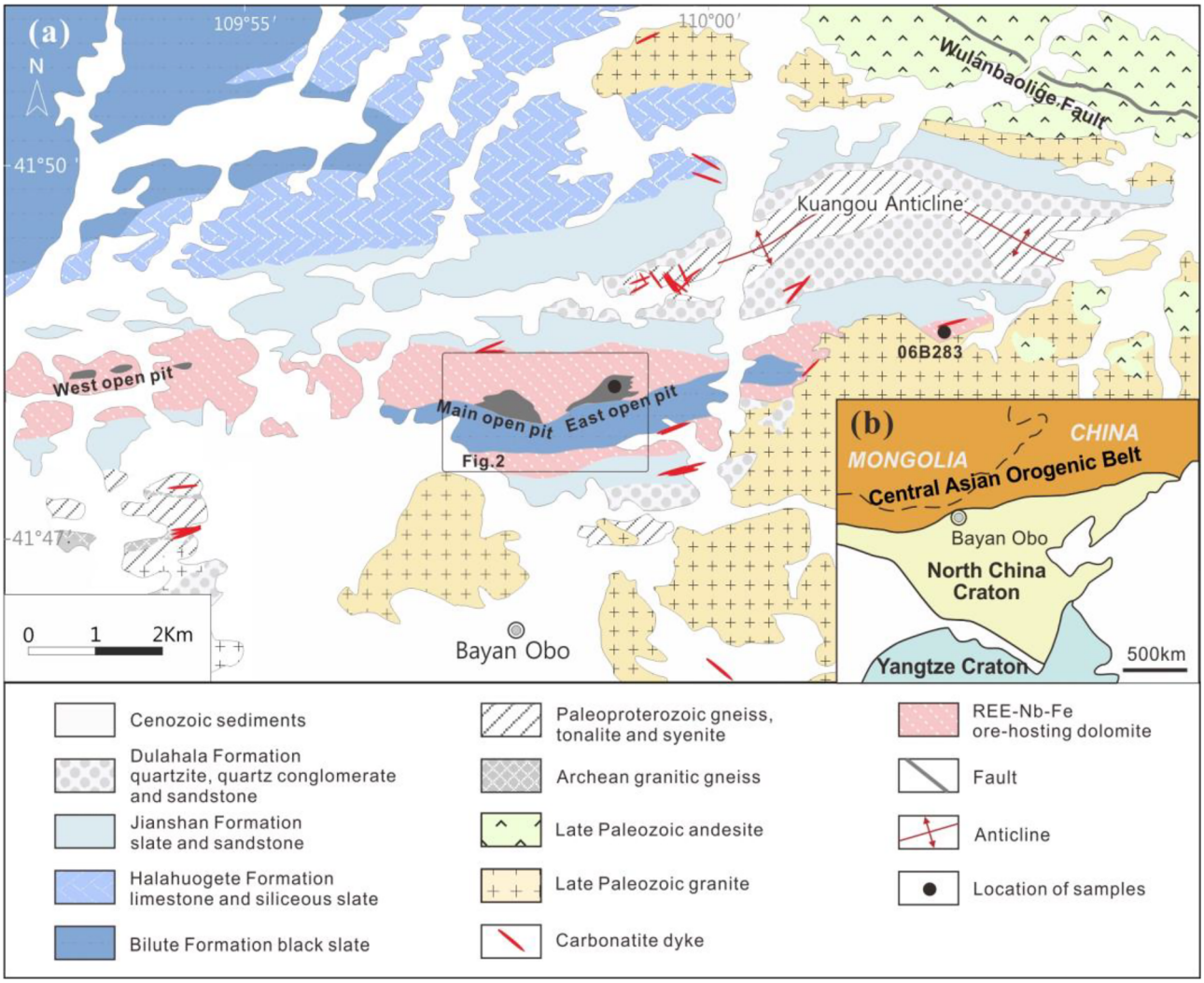

Fig. 1. Geological settings of the Bayan Obo REE-Nb-Fe deposit (modified after Yang et al. (2011a). Location of Bayan Obo in China has been marked in figure b). And the area of Fig. 2 has been represented by rectangle within.

largest Nb deposits worldwide, both related to fresh or weathered carbonatite, are Morro dos Seis Lagos deposit (2897.9 Mt@2.81% Nb_2O_5) and Araxá deposit (2608Mt@1.75% Nb_2O_5) in Brazil, respectively (Mackay and Simandl, 2014; Giovannini et al., 2017). The world-class Nb deposits are commonly accompanying with Ta, REE, W, Sn or P resources, but rather uncommon to accommodate REEs of comparable reservoir to Nb.

The Bayan Obo REE-Nb-Fe deposit is famous for its globally largest REE reservoir. Actually, it also hosts over 70% of China's current Nb resources, and contains many Nb-bearing minerals that were firstly discovered, such as fergusonite-(Ce) and baotite (Zhang et al., 2000; He et al., 2018). Although this deposit is characterized by large Nb ore tonnage with relatively low average Nb oxide grade (2.2 Mt@0.13% Nb_2O_5; Fan et al., 2016), Nb is heterogeneously distributed and locally enriched to 0.35 wt% of Nb_2O_5 in the ores (Zhang and Mu, 2006), comparable with some other valuable carbonatite-related Nb deposits. The origin of Nb has been assumed exactly the same as REEs at Bayan Obo, which originated from the Mesoproterozoic carbonatite melts (Smith and Spratt, 2012). However, the enrichment mechanism of Nb lacks detailed research, and the relationship between Nb and REE mineralization related with carbonatite has never been discussed properly. Since the distribution of Nb and REEs are not always coincident at Bayan Obo. For example, in most of the local carbonatite dykes, moderate REE enrichment is common while Nb-bearing minerals are rare (Wang et al., 2002; Yang et al., 2003, 2009, 2011a). In the metasomatized ore-hosting dolomite, diverse types of ores present relatively inconsistent preference for Nb or REE (Liu, 1985; Bai et al., 1996). Therefore, it is essential to explore the independent Nb behavior during the magmatic-hydrothermal evolution of carbonatite.

Various kinds of Nb-bearing minerals have been discovered in the Bayan Obo REE-Nb-Fe deposit, including aeschynite, pyrochlore, columbite, ilmenorutile, fergusonite, baotite, fersmite and so on. The aeschynite is the dominant Nb-bearing mineral in the Bayan Obo's ore-hosting dolomite, compared with pyrochlore, which is the major host for global carbonatite-related Nb resources (Cordeiro et al., 2011; Neumann and Medeiros, 2015; Hou et al., 2018). Complex Nb-bearing species imply complicated Nb precipitation process. Besides, the compositions of these Nb-bearing species vary significantly. According to the lanthanide fractionation and the Nb-Ti replacement in A and B lattice positions respectively, the aeschynite and fergusonite of Bayan Obo were classified into Ce-, Nd- and Y-rich species with Ti- or Nb-rich cations (Zhang and Tao, 1987; Yang et al., 2001). Variable compositions suggest evolving hydrothermal fluids or complex metasomatic process. In addition, in situ major and trace element analyses of Nb-bearing minerals have been recently used for recognition and portrayal of multistage magmatic-hydrothermal processes (Nasraoui and Bilal, 2000; Timofeev and Williams-Jones, 2015; Walter et al., 2018), which is urgent for further understanding of Nb mineralization at Bayan Obo.

Therefore, *in-situ* geochemical analyses, based on integral petrographic observation, are necessary to reveal the origin of Nb-bearing minerals and complex Nb enrichment processes.

There are dozens of geochronological works about the formation age of Bayan Obo carbonatite dykes, ore-hosting dolomite, local hydrothermal alteration and REE mineralization, which have been reviewed in Figs. S1 of Liu et al. (2020). Supported by Sm-Nd model ages of REE minerals and bulk ores, a Mesoproterozoic REE mineralization event related to carbonatite intrusion and a Paleozoic REE re-mobilization event related to subduction have been recognized (Hu et al., 2009; Yang et al., 2011). However, there has been no direct dating of Bayan Obo Nb-bearing minerals yet, which was simply regarded formed simultaneously to the REE minerals. Therefore, it is difficult to discuss the relationship between the Bayan Obo REE and Nb mineralization based on published dating results. Preliminary dating of aeschynite megacrysts would be introduced in this study, in order to provide direct geochronological constraint on the latest Bayan Obo Nb mineralization event.

This research aims to report petrography and geochemistry of various Nb-bearing minerals, interpret the origin of these minerals and the detailed process of Bayan Obo Nb mineralization, and attempt to figure out the relationship between Nb and REE enrichment in carbonatite-related magmatic-hydrothermal processes.

2. Geological settings

The Bayan Obo REE-Nb-Fe deposit is located on the north margin of the North China Craton (NCC) (Fig. 1). Archean and Paleoproterozoic metamorphic basement rocks are preserved in this region (Liu et al., 2011). During the breakup of Columbia Supercontinent, a series of Paleo-Mesoproterozoic (~1.8–1.4 Ga; Zhong et al., 2015; Liu et al, 2016) terrigenous sedimentary rocks, named as the Bayan Obo Group, developed on local rift basins. Subsequently, this sedimentary sequence was intruded by Mesoproterozoic carbonatite dykes (~1.4–1.2 Ga; Yang et al., 2011b; Fan et al., 2014). During the Paleozoic closure of the Paleo-Asian Ocean, both the basement and sedimentary rocks were folded and fractured extensively, and typical REE-rich vein-type of ores were formed simultaneously along extensional faults (Hu et al., 2009). Granite-diorite stocks intruded the Bayan Obo region, as response to the Permian continental collision between the NCC and the Siberian Craton (Fan et al., 2009). Since then, the geological settings of Bayan Obo have rarely been changed.

Majority of the REE-Nb-Fe resources are hosted in a nearly E-W-trending dolomite unit (Fig. 2a, d). The open pits, primarily designed to mine iron ore bodies, are extensively alkali-fluorine altered and REE-Nb mineralized as well (Fig. 2b, c). The major open pits include the East and Main open pits, and the currently largest West open pit. Besides, the entire dolomite unit, including the least altered dolomite outside the open pits, exhibits REEs and Nb backgrounds prominently higher than that of the average crust and the Bayan Obo Group, indicating a carbonatitic origin of REE and Nb (Liu et al., 2020). Carbonatite dykes intruding the Bayan Obo Group accommodate the rest of REE-Nb resources, with rare iron oxides (Yang et al., 2003). The sample locations and corresponding Nb-bearing minerals have been summarized in Table S1.

3. Methods

The backscatter electron imaging and energy dispersive spectrum analyses were conducted on a FEI Nova Nano SEM 450 scanning electron microscope, at the State Key Laboratory of Continental Dynamics, Northwest University, China. The acceleration voltage was set as 20.0 kV, with a probe diameter of 4 μm.

The electron microprobe analyses (EMPA) of Nb-bearing minerals were conduct on a JXA-8530F Plus at the State Key Laboratory of Nuclear Resources and Environment, East China University of Technology, China. The acceleration voltage was set as 15.0 kV, with a probe diameter of 2 μm. The natural and synthetic standard materials of analyzed elements are introduced as following: natural fluorite for F, tugtupite for Cl, olivine for Mg, jadeite for Al, almandine garnet for Si, niobate for Sr, barite or niobate for Ba, zirconia for Zr, rutile for Ti, calcite for Ca, magnetite for Fe, bustamite for Mn, synthetic phosphate ($REEP_5O_{14}$) for lanthanide series metals and Y, corresponding oxides for U, Th and Pb, and finally pure metals of Nb and Ta for these elements. All REEs have been analyzed for fergusonite. But only nine REEs have been analyzed for aeschynite and fersmite, e.g. La, Ce, Pr, Nd, Sm, Eu, Gd, Dy, Ho. None REEs have been analyzed for baotite and columbite.

In-situ REE and trace element components of Nb-bearing minerals were performed on thin sections under an Agilent 7700x, connected with the laser ablation system (GeoLasPro), at State Key Laboratory of Ore Deposit Geochemistry, China. The analytical laser beam has a diameter of 32 μm, energy density of 5 J and ablation frequency of 5 Hz. Nitrogen was applied as the carrier gas. The sample ablating time was set to 40 s and the entire time of each run was set to 90 s. NIST-610 was selected as external standard material since there is no available international standard material of Niobium oxides. Considering potential problem with absolute concentration, these analytical results were only used to calculate REE patterns, Y/Ho and Nb/Ta ratios. Each 10–15 spot analyses of Nb-bearing minerals were followed by two international standard material analyses. Ti was set as the internal standard of aeschynite, ilmenorutile and baotite which has been formerly analyzed by EMPA. The internal standard of fersmite was set to Ca. The trace and REE element composition (e.g. content of Y, Nb, Ba, lanthanides, Ta, Th and U) was calculated and corrected with assistance of software ICPMSDataCal v10.7 (Liu et al., 2008).

Aeschynite monominerals were collected from 7 samples that contain megacrysts of aeschynite under the binocular. The grinded aeschynite was then dissolved in $HClO_4$-HNO_3-HF acid solution. It is noticeable that new white sandy precipitate was formed at the bottom of Teflon vessels when HF was expelled before sample introduction to the ICP-MS, and there is no former research mentioned this phenomenon. The white precipitate should be pure Nb_2O_5, whose solubility is sensitive to HF activity in solution (Timofeev et al., 2015), which is significantly distinct from the original semitransparent dark brown aeschynite ($[REE,Ca](Nb,Ti)_2O_6$) powder. The trace element analyses of these aeschynite monominerals were performed on an Agilent ICP-MS 7700 at Key Laboratory of Mineral Resources in Western China (Gansu Province), Lanzhou University. The external standard material is BCR-2, and all analytical results were calibrated against a set of multi-element standard solutions. Solution of all 7 samples contains extremely high REE and Ti content, with Nb composition 1–3 orders of magnitude lower than chemical formula of these aeschynite (analyzed by EMPA), furtherly demonstrating that the new precipitate is pure niobium pentoxide.

For each sample, 100 mg aeschynite powder was decomposed in a mixture of $HClO_4$-HNO_3-HF in the Teflon vessels. Sm-Nd and Rb-Sr were separated from the solution using resin AG 50 W-X12 and HDEHP-coated Teflon powder, respectively. $^{87}Rb/^{86}Sr$ and $^{143}Sm/^{144}Nd$ ratios were calculated with formerly ICP-MS-analyzed Rb, Sr, Sm and Nd composition, and with newly measured $^{87}Sr/^{86}Sr$ and $^{143}Nd/^{144}Nd$. Rb-Sr and Sm-Nd isotopes were analyzed on a Finnigan MAT 262 TIMS at University of Science and Technology of China. In these analyses, the $^{87}Sr/^{86}Sr$ ratios were normalized to $^{86}Sr/^{88}Sr = 0.1194$ and the $^{143}Nd/^{144}Nd$ ratios to $^{146}Nd/^{144}Nd = 0.7219$. The Nd standard solution (La Jolla) has $^{143}Nd/^{144}Nd$ ratio of 0.511869 ± 6 (2σ) and the Sr standard (NBS 987) has $^{87}Sr/^{86}Sr$ ratio of 0.710249 ± 12 (2σ). Detailed description of sample preparation for the isotopic analyses has been published in Chen et al. (2000, 2007).

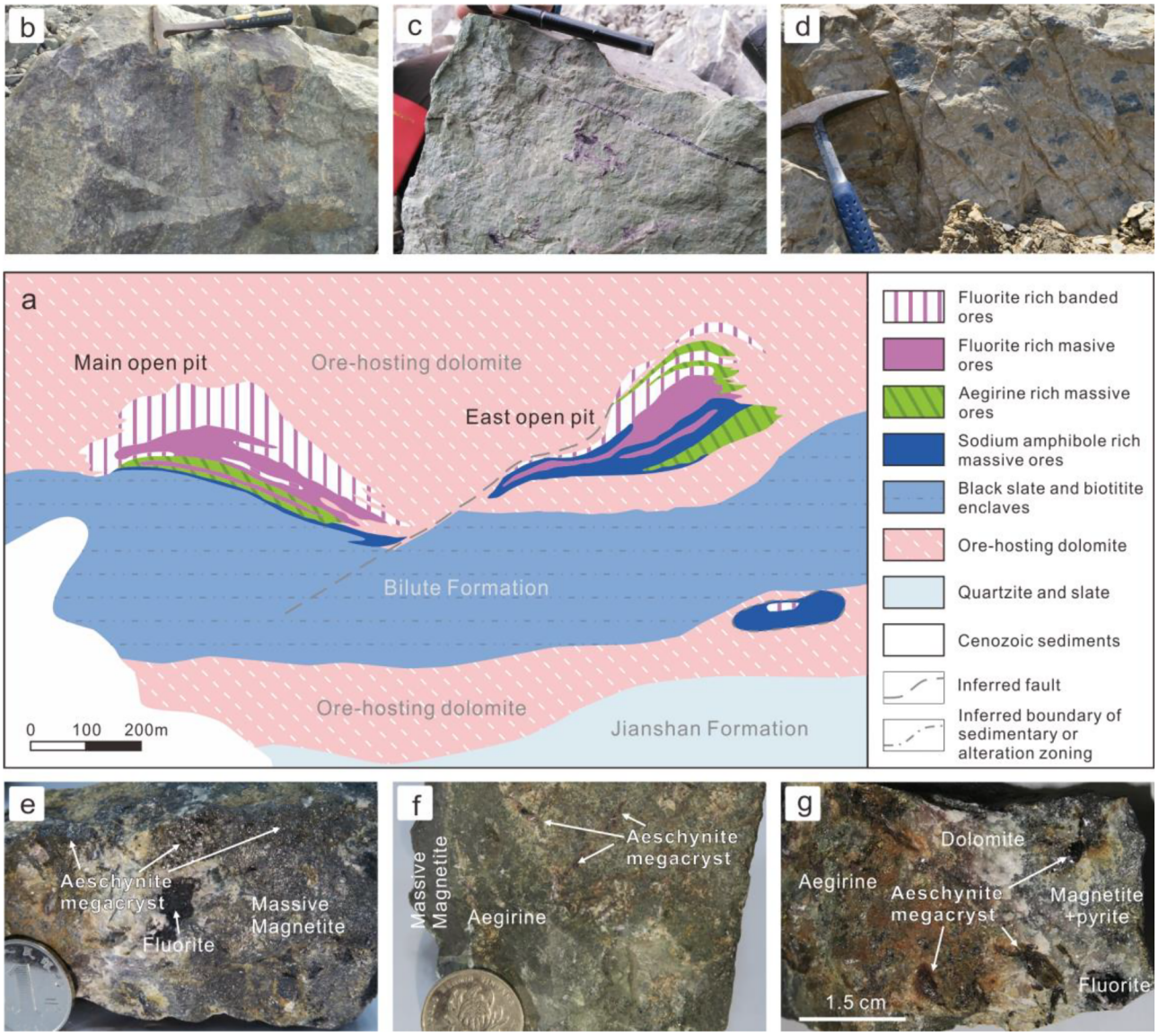

Fig. 2. Typical ores or ore-hosting dolomite with Nb-bearing minerals a) the typical ore zonation inside the East and Main open pits (adapted from IGCAS (1988)); b) field photography of fluorite-rich massive ores; c) field photography of aegirine-rich massive ores; d) the slightly-altered ore-hosting dolomite with slate enclaves from the Bayan Obo Group; e) dark brown aeschynite megacrysts in the massive REE-Fe ores (19BY03); f) aeschynite megacrysts (dark brown long prismatic minerals) in the aegirine-rich REE-Fe ores (19BY05); g) aeschynite megacrysts in the aegirine-rich REE-Fe ores (19BY07). Nb-bearing minerals are invisible in field photography.

4. Petrography

4.1. Aeschynite

Aeschynite is one of the most common Nb-bearing minerals at Bayan Obo. Aeschynite was observed from 16 samples, including fluorite-rich REE-Fe ores (No. 17BY04, 17BY31, 17BY37), sodium-amphibole-rich REE-Fe ores (17BY135, 17BY136), aegirine-rich REE-Fe ores (17BY197), slightly-altered ore-hosting dolomite (14BY4-15), and vein-type of ores or veinlets cutting through the above ores (14BY2-25, 14BY4-13, 19BY02-19BY07, 16BY29).

In the fluorite-rich REE-Fe ores (No. 17BY04, 17BY31, 17BY37), aeschynites are interstitial to magnetite aggregates (17BY04, 17BY31-2; Fig. 3a) or intercepted by megacrysts of iron oxides and sodium amphiboles successively (17BY37; Fig. 3b). In sample 17BY31-3, biotite and dolomite matrix were the relatively earlier formed minerals, in which the fine-grained aggregates of aeschynites occasionally replaced monazite of similar grain size, then replaced by megacrysts of iron oxides (Fig. 3c, d).

In the sodium-amphibole-rich REE-Fe ores (17BY135, 17BY136), aeschynite crystallized among magnetite crystals along the mica-fluorite vein (17BY135-1; Fig. 3e) or replaced phlogopite among magnetite grains (Fig. 3f), or associated with chevkinite and then corroded fluorite and micas (17BY135-3; Fig. 3g), or replaced sodium amphibole, fluorite and their associated bastnaesite and thorite, then intercepted by sub-euhedral iron oxides crystals (17BY136; Fig. 3h).

In aegirine-rich REE-Fe ores (17BY197), an aeschynite crystal with complex annulus is surrounded and corroded by dolomite and apatite (Fig. 3i). The darker annulus in BSE images may have been hydrated. Similarly, in the slightly-altered ore hosting dolomite (14BY4-15), anhedral aeschynite has also been hydrated with similar dark rim (Fig. 3j). Moreover, sample 14BY4-15 contains orientated aggregates of monazite, fluorite, quartz and iron oxides, in the direction of lineation of these aeschynites, excluding their primary origin.

Aeschynite megacrysts in the vein-type of ores (14BY4-13, 19BY02-19BY07) are generally associated with calcite aggregates, but barely

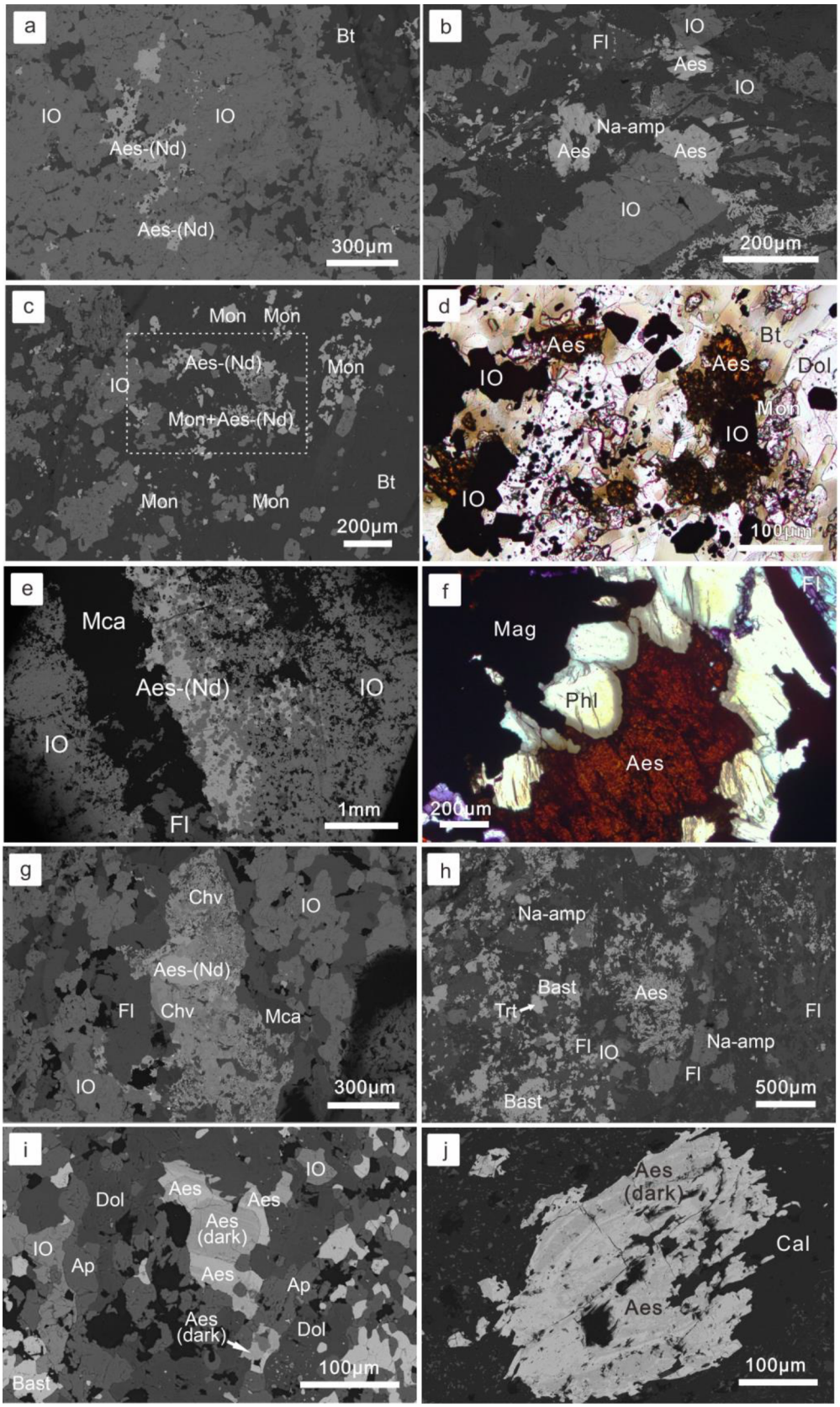

Fig. 3. Petrography of aeschynite in fluorite-rich REE-Fe ores, sodium-amphibole-rich REE-Fe ores, aegirine-rich REE-Fe ores and slightly-altered ore-hosting dolomite, Bayan Obo. a) interstitial aeschynite between iron oxides in the fluorite-rich ore, BSE images of 17BY31; b) aeschynite is associated with fluorite, and replaced by iron oxides and sodium amphibole in the fluorite-rich ores, BSE image of 17BY37; c) fine-grained aeschynite replaced monazite, BSE image of 17BY31; d) image of box in c), shot under plane polarized light; e) aeschynite crystalized along the mica-fluorite vein cutting through the sodium-amphibole-rich REE-Fe ores, BSE image of 17BY135; f) aeschynite megacryst has been corroded by phlogopite in the sodium-amphibole-rich ores, 17BY135 under plane polarized light (ppl); g) aeschynite is associated with chevkinite and surrounded by fluorite and iron oxide, BSE image of 17BY135; h) aeschynite and bastnaesite were replaced by sodium amphiboles and fluorite in the sodium-amphibole-rich ores, BSE image of 17BY136; i) in aegirine-rich REE-Fe ores, aeschynite with complex annulus is surrounded and corroded by dolomite and apatite, BSE image of 17BY197; j) aeschynite with dark rims in the slightly-altered ore-hosting dolomite, BSE image of 14BY4-15. Abbreviation of minerals: Aes-aeschynite, IO-iron oxides, Bt-biotite, Fl-fluorite, Na-amp-sodium amphibole, Mca-mica, Phl-phlogopite, Mag-magenetite, Chv-chevkinite, Trt-thorite, Bast-bastnaesite, Dol-dolomite, Cal-calcite, Ap-apatite.

associated with REE-minerals (fluorocarbonates and monazite), which are common in typical REE-rich vein-type of ores. Other associated minerals include megacrysts of fluorite, pyrite, iron oxides and barite, with aggregates of sodium amphibole or aegirine. Euhedral aeschynite megacrysts are also discovered in the aegirine-rich REE-Fe ores or massive REE-Fe ores (Fig. 2e–g). The aeschynite in sample No. 14BY4-13 envelops euhedral sodium amphiboles (long prismatic crystals with developed cleavages along b axis), and has been corroded by

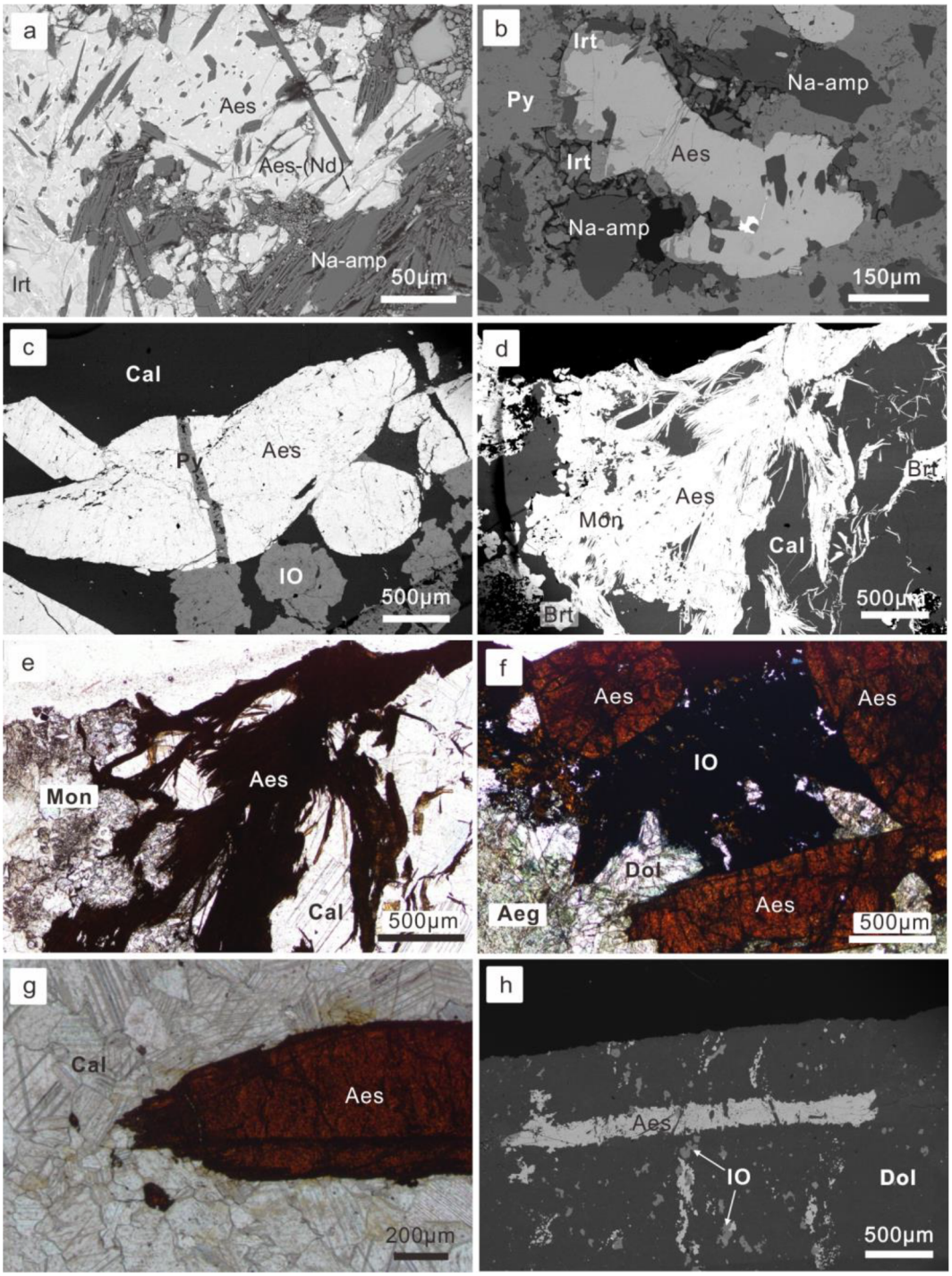

Fig. 4. Petrography of aeschynite in the vein-type of ores or veinlets cutting through other kinds of ores, Bayan Obo a) aeschynite that is associated with sodium amphibole, and aeschynite-(Nd) surrounding the sodium amphibole inclusions, BSE image of 14BY4-13; b) aeschynite is rimmed by ilmenorutile and surrounded by pyrite and amphiboles, BSE image of 14BY2-25; c) aeschynite megacryst cut by pyrite veinlet, BSE image of 19BY03; d-e) fibrous aeschynite aggregates associated with barite, d) is BSE image of 19BY04, e) was captured under ppl; f) euhedral aeschynite in the massive aegirine-rich ores, 19BY05 under ppl; g) euhedral aeschynite in calcite vein, 19BY07 under ppl; h) aeschynite vein in the sodium-amphibole-rich ores, BSE image of 16BY29. Abbreviation of minerals: Irt-ilmenorutile, Py-pyrite, Mon-monazite, Brt-barite. Other abbreviations are the same as those in above figures.

surrounding sodium amphibole aggregates (Fig. 4a). Therefore, aeschynites in this sample were formed simultaneously to the sodium amphiboles. Aeschynite in sample No. 14BY2-25 is rimmed by ilmenorutile and surrounded by pyrite and amphiboles (Fig. 4b), aeschynite megacryst in 19BY03 is cut by pyrite veinlet (Fig. 4c), and fibrous aeschynite aggregates in 19BY04 are associated with barite and replaced fine-grained monazite aggregates (Fig. 4d, e). Euhedral aeschynite in 19BY05 and 19BY06 replaced massive aegirine-rich ores (Fig. 4f). The rest of aeschynites in the vein-type of ores are presented as discrete euhedral prismatic megacrysts in the calcite-dominated veins, as in 19BY02 and 19BY07 (Fig. 4g). Thus, the aeschynite in the vein-type of ores was one of the last formed minerals during the Paleozoic hydrothermal activities. In general, aeschynites in the vein-type ores are rarely associated with other REE-rich minerals, except 19BY04, in

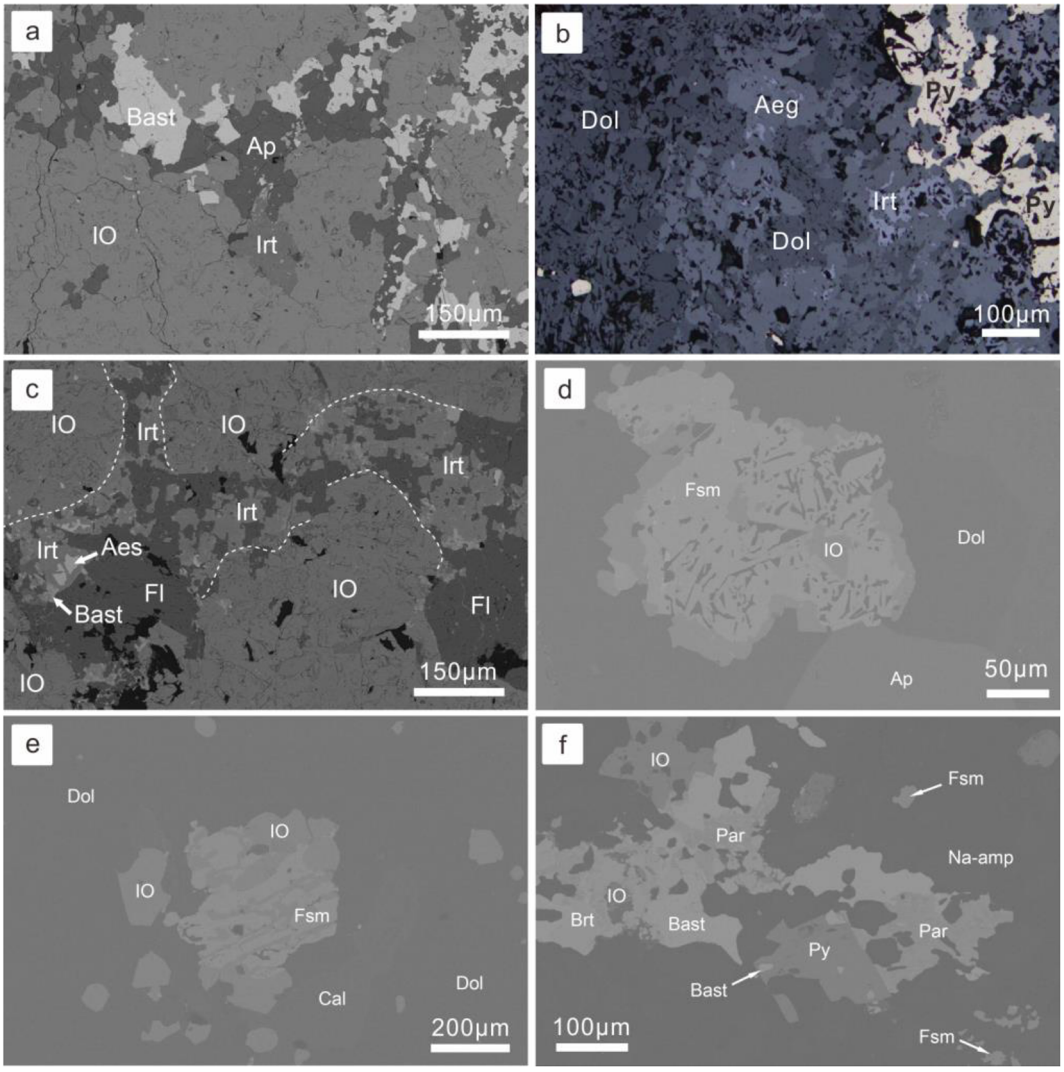

Fig. 5. Petrography of ilmenorutile and fersmite in different kinds of ores and the ore-hosting dolomite, Bayan Obo a) ilmenorutile associated with apatite and micas in aegirine-rich REE-Fe ores, BSE image of 17BY179; b) ilmenorutile associated with pyrite in aegirine-rich ore-hosting dolomite, image of 15BY99 under reflection light; c) interstitial ilmenorutiles, with aeschynite inclusions, crystallized among iron oxide crystals in the fluorite-rich REE-Fe ores, BSE image of 17BY04; d) fersmite replaced by iron oxides in coarse-grained ore-hosting dolomite, BSE image of 06B283; e) fersmite associated with iron oxides in the same sample as d), BSE image; f) discrete anhedral fersmite in fine-grained ore-hosting dolomite, BSE image of 05B184. Abbreviation of minerals: Irt-ilmenorutile, Aeg-aerigine, Fsm-fersmite, Par-parisite. Other abbreviations are the same as those in above figures.

which aeschynite replaced monazite aggregates. In the weakly-altered dolomite (16BY29), there is aeschynite veinlet cutting through it (Fig. 4h).

4.2. Ilmenorutile

Ilmenorutile was occasionally observed in our samples. For example, the ilmenorutile is associated with iron oxides, apatite and micas in aegirine-rich REE-Fe ores (17BY197; Fig. 5a), associated with pyrite in aegirine-rich ore-hosting dolomite (15BY99; Fig. 5b), or present as interstitial ilmenorutile veins among magnetite aggregates in the fluorite-rich REE-Fe ores (17BY04; Fig. 5c), associated with fluorite and containing aeschynite inclusions. Besides, aeschynite in 14BY2-25 has ilmenorutile rim, which also indicate that the ilmenorutile crystallized postdating the aeschynite during the Paleozoic hydrothermal activities.

4.3. Fersmite

Fersmite has been rarely observed in our samples. However, there is close association of fersmite and iron oxides in the coarse-grained ore-hosting dolomite (sample No. 06B283; Fig. 5d, e). With assistance of energy disperse spectroscopy, partial “fersmite” crystals in the same sample are actually columbite-(Mg) with similar brightness as that of fersmite in BSE images. The ‘wormlike’ Ca-rich Nb oxides (fersmite, $CaNb_2O_6$) and Mg-Fe-rich Nb oxides (columbite-(Mg), $(Mg_{0.5}Fe_{0.4}Mn_{0.1})_{1.0}Nb_2O_6$) replaced the dolomite host and were then replaced by iron oxides from the margins or fractures of fersmite aggregates. Discrete anhedral fersmite grains were also observed in the fine-grained ore-hosting dolomite (sample No. 05B184; Fig. 5f). In general, fersmite is rare in extensively metasomatized ore-hosting dolomite or ores observed in this study.

4.4. Columbite

Columbite is also rare compared with other Nb oxides, such as aeschynite and ilmenorutile. However, there is columbite in the aegirine-rich REE-Fe ores (sample No. 17BY06; Fig. 6a) associated with anhedral barite, which has been regarded to have a Paleozoic hydrothermal origin. Besides, columbite also crystallized among fine-grained monazite and iron oxide in the apatite-rich REE-Fe ores (sample No.

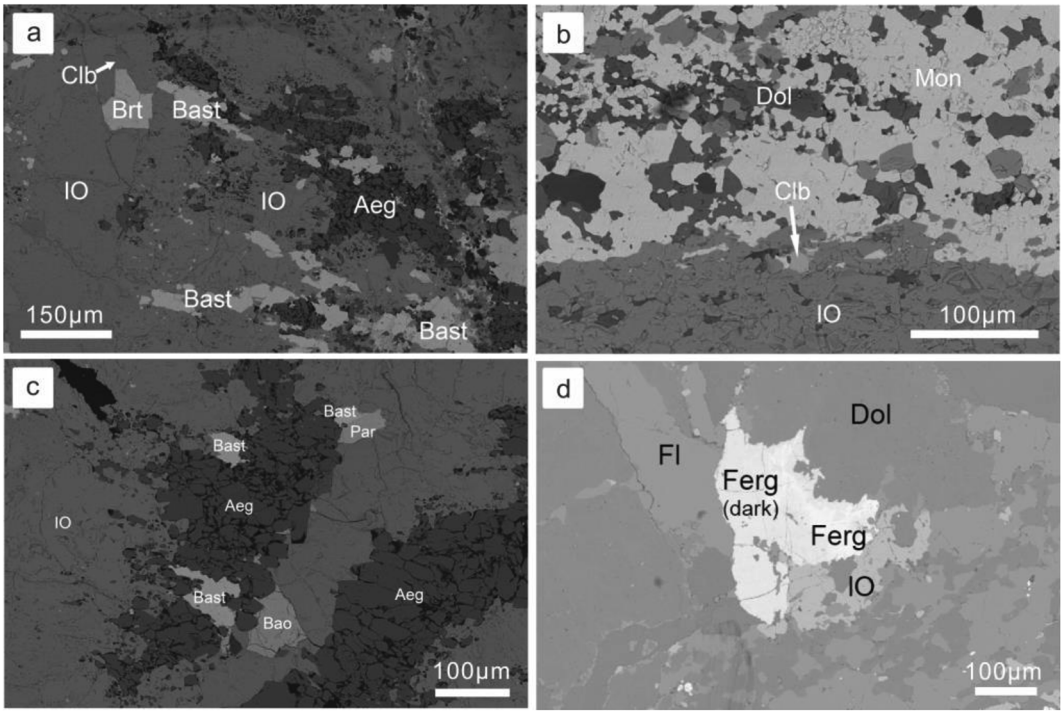

Fig. 6. Petrography of columbite, Baotite and fergusonite in different kinds of ores and the ore-hosting dolomite, Bayan Obo a) columbite associated with anhedral barite in the aegirine-rich REE-Fe ores, BSE image of 17BY06; b) columbite at the boundaries between aggregates of iron oxides and monazite, in the apatite-rich REE-Fe ores, BSE image of 17BY196; c) anhedral baotite filling fractures of aggregates of aegirine and iron oxides, in the aegirine-rich REE-Fe ores, BSE image of 17BY06; d) fergusonite with dark rims in the fluorite-rich ore-hosting dolomite, BSE images of 14BY3-4. Abbreviation of minerals: Clb-columbite, Bao-baotite, Ferg-fergusonite. Other abbreviations are the same as those in above figures.

17BY196; Fig. 6b). Both the monazite and iron oxide aggregates are directionally aligned, indicating these minerals were crystallized under prominent stress. Moreover, a few discrete euhedral columbite grains have been observed in the fine-grained ore-hosting dolomite (sample No. 05B184).

4.5. Baotite

Baotite was firstly discovered at Bayan Obo and was named after the nearest city of Baotou. This kind of mineral seems to prefer aegirine-rich REE-Fe ores (sample No. 17BY06, 17BY10) as host rock, filling fractures of iron oxides and aegirine aggregates (Fig. 6c). Baotite presents as pale yellow–brown transparent crystals under the plane polarized light. These anhedral baotite crystals are shaped and restricted by the cleavages of the iron oxides, indicating the baotite crystallized postdating the formation of aegirine-rich ores, which has definite hydrothermal origin.

4.6. Fergusonite

Fergusonite-(Y) has been observed in the fluorite-rich dolomite (sample No. 14BY3-4), with dark brown color under plane polarized light. It replaced fluorite vein and micas slabs, eroding both the later-formed iron oxides and the earlier-formed dolomite matrix compared with fluorite and micas (Fig. 6d). Thus, fergusonite-(Y) is the latest crystallized minerals in the fluorite-rich dolomite, even after the Paleozoic formation of micas. It is also noticeable that the margin of the fergusonite has been altered and presents lower brightness in BSE images. This phenomenon indicates the decrease of average atomic weight of the margin, may due to the introduction of more hydroxyl and fluorine during the hydration reaction.

The petrogenesis of the mentioned minerals has been summarized in Fig. 7 and there is detailed description in the discussion.

5. Analytical results

5.1. Major elements of Nb-bearing minerals

Aeschynite (AB_2O_6) group minerals in Bayan Obo contain Nb and Ti cations in B site and LREE (mainly Ce, Nd and Sm) cations in A site (Fig. 8). According to nomenclature of aeschynite based on Ce/Nd and Ti/Nb ratios (Yang et al., 2001; Bermanec et al., 2008), aeschynite with Ti or Nb as dominating cation in B site was named as “aeschynite” and “nioboaeschynite” respectively, with suffix of “-Ce”,“-Nd” or “Y” when its corresponding concentration exceeds the rest of REEs. The chemical structures of aeschynite have been calculated in 6 oxygen atoms per formula (Table 1; Whole list in Table S2). The EMPA results show that aeschynite in the fluorite-rich or sodium-amphibole-rich REE-Fe ores, and those aeschynite megacrysts in the vein-type of ores generally have Ce/Nd ratios < 1. Meanwhile, small portion of aeschynite in the vein-type of ores (19BY04), and almost all aeschynite in the aegirine-rich REE-Fe ores and the slightly-altered ore-hosting dolomite contain more Ce than Nd in chemical formulas. As for Ti/Nb ratios of aeschynite, regardless of the ore types of host rocks, most analyzed aeschynites belong to “aeschynite” rather than “nioboaeschynite”, except those in the slightly-altered ore-hosting dolomite and those in sample 14BY2-25 (pyrite-sodium-amphibole vein) that relatively lack of Ti. The EMPA results also show that partial aeschynite in the fluorite-rich REE-Fe ores, slightly-altered ore-hosting dolomite and vein-type of ores, as well as nearly all analyzed aeschynite in aegirine-rich REE-Fe ores contain sum weight < 100%, may due to epigenetic alteration or because some major elements have been missed during EMPA, which are likely to be the undetected REEs. Therefore, accurate analyses of whole lanthanides in different aeschynite were then performed on a LA-ICPMS.

Based on limited published EMPA data, only half of the lanthanides (La, Ce, Pr, Nd, Sm, Eu, Gd, Dy) in Bayan Obo aeschynite have concentration far above the detection limit of EMPA, thus not all lanthanides were analyzed (IGCAS, 1988; Yang et al., 2001; Smith and Spratt,

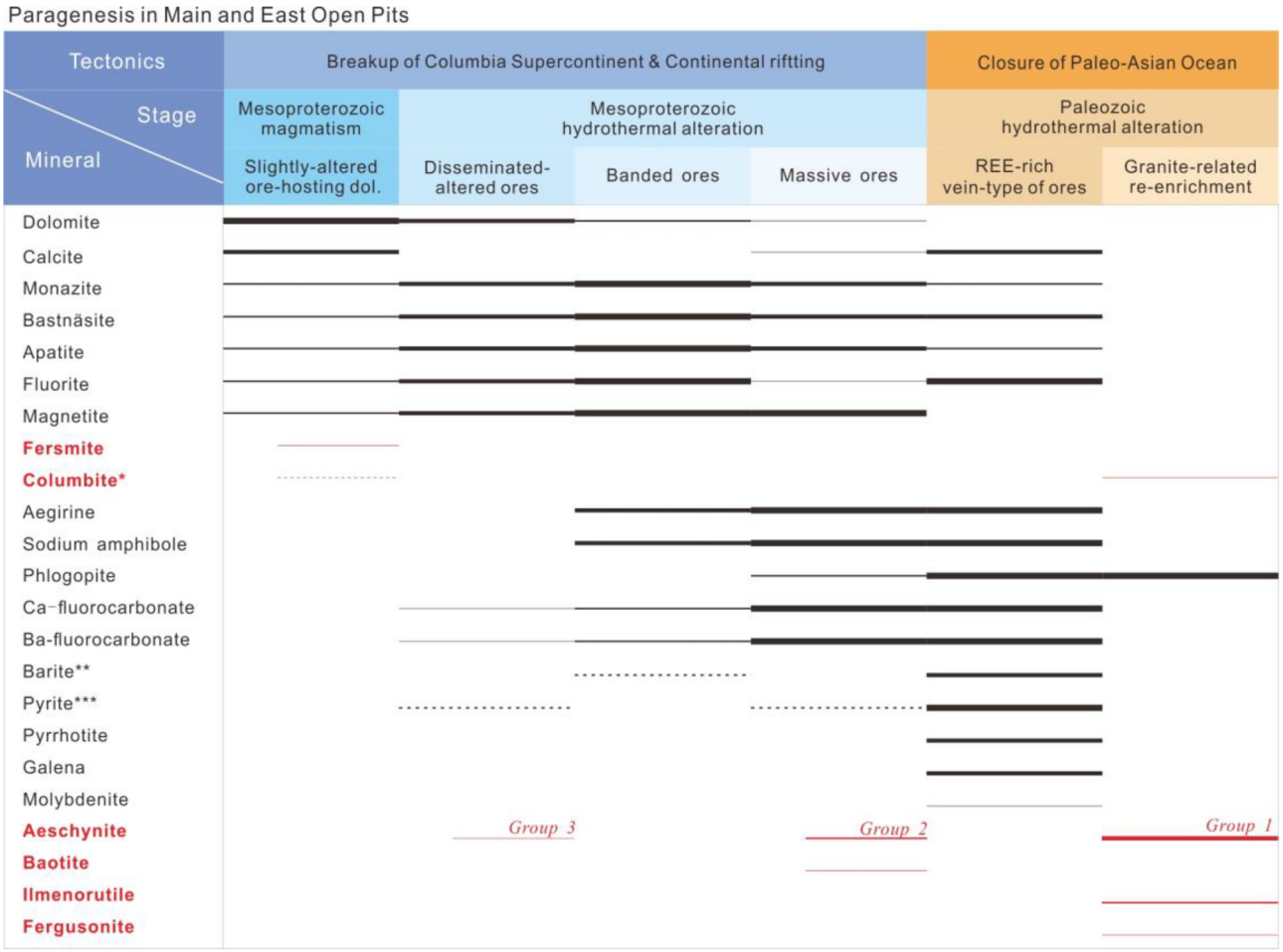

Fig. 7. Petrogenesis of common minerals in the ores and ore-hosting dolomite, East and Main open pits of the Bayan Obo REE-Nb-Fe deposit (Modified after Liu et al. (2018a) *Igneous columbite with dash line is summarized according to Le Bas et al. (1992). **Barite was occasionally observed in the banded ores. However, these barites are regarded to have similar origin as barite in the Paleozoic vein-type of ores. ***Pyrite is a kind of characteristic Paleozoic gangue mineral in the Bayan Obo ore and ore-hosting dolomite, regardless of its occurrence, because of similar S isotope (Liu et al., 2018b).

2012). The ΣLREO (light rare earth element oxides) of these aeschynite would be presented hereto according to EMPA. As for ΣLREO, the unaltered aeschynite in the fluorite-rich REE-Fe ores contain ΣLREO of 16 wt%–32 wt%, mostly between 24 wt% and 32 wt%, more than the altered aeschynite in the same type of ores, with ΣLREO of 16 wt%–19 wt%. The aeschynite in the sodium-amphibole-rich REE-Fe ores (ΣLREO: 24 wt%–30 wt%), slightly-altered ore-hosting dolomite (ΣLREO: 23 wt%–28 wt%) and vein-type of ores ((ΣLREO: 22 wt%–29 wt%) has ΣLREO in the range of the unaltered aeschynite in fluorite-rich ores. While aeschynite in the aegirine-rich ores contain REE oxides of 8 wt%–23 wt%, similar to the altered aeschynite in the fluorite-rich ores. The classification of Bayan Obo aeschynite would be described in the following section, combined with REE and trace element characteristics.

Ilmenorutile ($(Ti,Nb,Ta,Fe)O_2$) is also termed as niobian rutile (Silvola, 1970). Ilmenorutile in the aegirine-rich REE-Fe ores (17BY197; 15BY99) have formula between $(Ti_{0.96}Nb_{0.02}Fe^{2+}_{0.02})_{1.00}O_2$ and $(Ti_{0.89}Nb_{0.06}Fe^{2+}_{0.06})_{1.01}O_2$. However, interstitial ilmenorutile veins in the fluorite-rich REE-Fe ores (17BY04) contain sum weight far < 100 wt%, indicating extensive element exchange or epigenetic hydration (Table 2).

Fersmite ($CaNb_2O_6$) in the slightly-altered ore-hosting dolomite (06B283; 05B184) has a formula of $(Ca_{0.96}Mg_{0.02}Mn_{0.01})_{0.99}(Nb_{1.93}Ta_{0.03}Fe^{3+}_{0.02})_{1.98}O_6$, which is rather close to the ideal chemical formula. Fersmite in 05B184 may have total weight as low as 96.13 wt%, with small amount of F^- in the lattice, indicating alteration by fluorine-rich fluids (Table 3; Whole list in Table S3).

Analyzed columbite ($FeNbO_4$) in Bayan Obo has significantly varying major components (Table 4; Whole list in Table S4). Columbite grains in the apatite-rich REE-Fe ores (sample No. 17BY196) have a formula of $(Mn_{0.87}Fe^{2+}_{0.22})_{1.09}(Nb_{1.93}Ti_{0.01})_{1.94}O_6$ if calculating in 6 oxygen atoms, which belongs to columbite-(Mn), or Manganocolumbite, according to the nomenclature of Černý and Ercit (1989) and Tindle and Breaks (2000). While columbite in the fine-grained ore-hosting dolomite (sample No. 05B184) has different major components, with chemical formula of $(Fe^{2+}_{0.84}Mn_{0.20}Mg_{0.03})_{1.07}(Nb_{1.90}Ti_{0.09})_{1.99}O_6$. These columbite grains was named as columbite-(Fe) or ferrocolumbite. Columbite in the third sample, coarse-grained ore-hosting dolomite (sample No. 06B283), presents distinct major components compared with the former grains, with chemical formula of $(Mg_{0.54}Fe^{2+}_{0.37}Mn_{0.11}Ca_{0.01})_{1.03}(Nb_{1.95}Ta_{0.03})_{1.98}O_6$, which should be named as columbite-(Mg) or Magnocolumbite. The columbite-(Mg) contains Ta_2O_5 between 1.41 and 2.71 wt%, while Ta_2O_5 content of the other two kinds of columbite was undetectable by EMPA. In addition, columbite-(Mg) is closely associated with fersmite and iron oxides. Fersmite in the same sample (06B283) present average chemical formula of $(Ca_{0.97}Ce_{0.02}La_{0.01}Nd_{0.01}Mg_{0.01}Mn_{0.01})_{1.03}(Nb_{1.93}Ta_{0.03}Fe^{3+}_{0.02})_{1.98}O_6$. It is noticeable that the Ta could only be detected in columbite-(Mg) and fersmite in sample No. 06B283.

Baotite ($Ba_4Ti_8Si_4O_{28}Cl$) at Bayan Obo is special for its significant Nb content, which has been found in carbonatite or lamproite dykes (Cooper, 1996; Kullerud et al., 2012). The chemical formulas of baotite

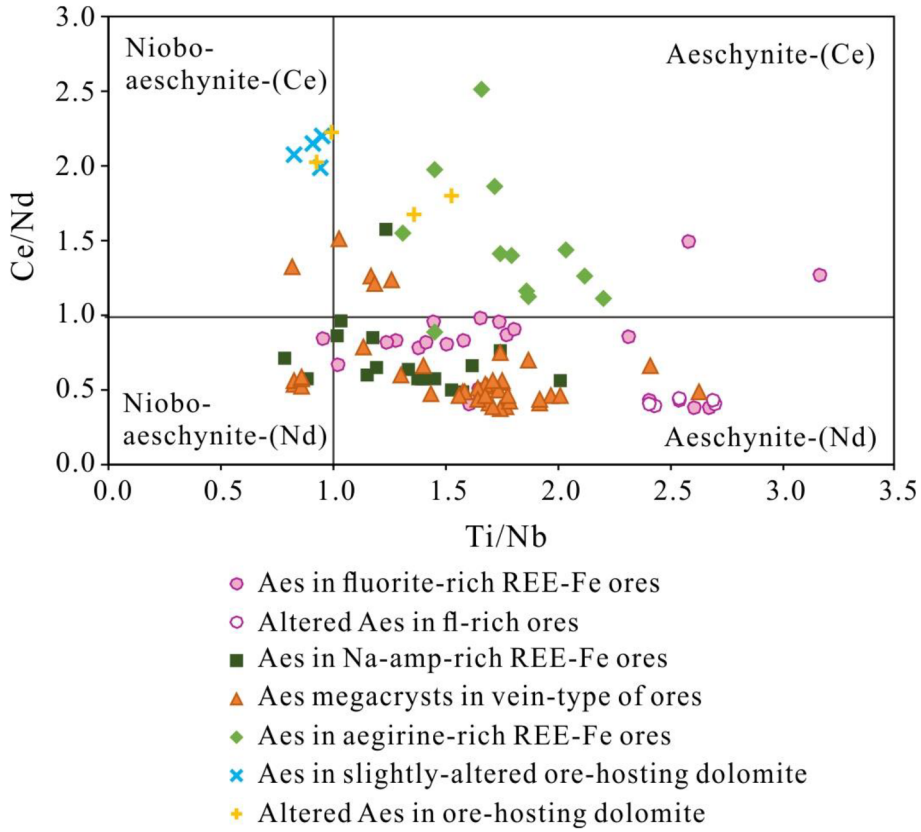

Fig. 8. Major element composition and classification of aeschynite (Aes).

in the aegirine-rich REE-Fe ores are $(Ba_{3.96}Sr_{0.04})_{4.00}(Ti_{4.62}Nb_{2.02}Fe^{2+}_{1.27})_{7.91}Si_{3.76}O_{27.09}Cl_{1.02}$ (sample No. 17BY06) and $(Ba_{4.08}Sr_{0.02})_{4.10}(Ti_{5.26}Nb_{1.70}Fe^{2+}_{0.94})_{7.91}Si_{3.82}O_{27.49}Cl_{0.93}$(17BY10), if calculating in 16 cations of the formula (Table 5).

Fergusonite ($REENbO_4$) at Bayan Obo is characterized by Yttrium that plays as the dominating REE in lattice (Table 6; Whole list in Table S5). Analyzed fergusonite comes from the fluorite-rich ore-hosting dolomite (14BY3-4), with dark rims in BSE images. The brighter core is unaltered with F < 0.01 wt% and Nb_2O_5 > 45.2 wt%. Meanwhile, the dark rim contains more Si, Mn, Fe, Th cations and more F replacing the oxygen atoms, with decreased Nb_2O_5 (42.0 wt%–43.4 wt%) and Y_2O_3. All analyzed fergusonite spots, both on the core and the altered rim, present unique LREE-depleted and HREE-enriched chondrite-normalized REE patterns.

5.2. REE and trace elements analyzed by (LA ±) ICP-MS

In-situ REE and trace element analyses have been conducted on aeschynite, ilmenorutile, fersmite and baotite (Table 7; Whole list in Table S6). The chondrite normalized REE patterns were calculated and plotted based on these in-situ REE concentration (Fig. 9).

Based on the major and rare earth elements obtained by EMPA and LA-ICPMS, the Bayan Obo aeschynite in this study was generally divided into three groups. Group 1: Aeschynite-(Nd), the major kind of aeschynite, which is characterized by dominating Nd and Ti cations in the A and B sites of aeschynite, with relatively high ΣLREO components (16%–32%) and convex chondrite-normalized REE patterns, relatively lacks La and HREEs. Almost all aeschynite in the fluorite-rich and sodium-amphibole-rich REE-Fe ores, and most of aeschynite megacrysts in the vein-type of ores belong to this group. As exception, the altered aeschynites in the fluorite-rich ores keep similar Nb/Ti, Ce/Nd ratios and REE patterns to the unaltered, with prominent decrease of ΣLREO (16 wt%–19 wt%). Group 2: Aeschynite-(Ce), which contains more Ce than Nd in A site, with relatively lower ΣLREO components (8 wt %–25 wt%). Aeschynite in the aegirine-rich ores belong to this group. Although with lower ΣLREO, aeschynite in the aegirine-rich ores present nearly flat REE patterns. In addition, aeschynite vein cutting through the ore-hosting dolomite also belongs to this group (19BY04). Group 3: Nioboaeschynite, which contain more Nb in B sites of aeschynite lattice, with relatively high ΣLREO components (25 wt %–28 wt%). Aeschynite in the slightly-altered ore-hosting dolomite belongs to this group, presenting flat LREE-MREE patterns that lack of HREE, with generally higher Ce/Nd ratios than aeschynite of Group 1 with similar convex REE patterns. As exception, megacrysts of aeschynite in a pyrite-sodium-amphibole vein (14BY2-25) also belong to this group but with Nd as dominating REE cation.

Ilmenorutile has the most variable ΣREE and REE patterns, including convex patterns with high ΣREE and right-downward patterns with moderate to low ΣREE (Fig. 9f). Fersmite presents consistently LREE-enriched patterns. Finally, fergusonite prefers to carrying HREE and therefore exhibits unique HREE-enriched patterns compared with the rest of Nb-bearing minerals (Fig. 9g). Baotite lacks REEs except Gd and its REE pattern would not be furtherly discussed.

All analyzed Bayan Obo aeschynite grains contain Y/Ho ratios (8.6–21.0) lower than the primitive mantle (PM) Y/Ho ratios (27.7 for Sun and McDonough (1989) and 28 ± 3 for Bau (1996)). It is noticeable that aeschynite (Group 2 and 3) in the aegirine-rich REE-Fe ores (8.6–11.5) and slightly-altered ore-hosting dolomite (9.9–14.3) present relatively lower Y/Ho ratios, which was caused by HREE enrichment in these aeschynite. Nb-Ta fractionation is very prominent in aeschynite, ilmenorutile and baotite with extremely high Nb/Ta ratios (1163–107229). Specifically, aeschynite in the aegirine-rich REE-Fe ores (1313–2853) and slightly-altered ore-hosting dolomite (1950–3254) present relatively lower Nb/Ta ratios, due to relatively enriched Ta (Aes. Group 2&3: 109.6–331.3 ppm) compared with aeschynite hosted in other types of ores (Aes. Group 1: < 100 ppm).

Table 1
Major element composition of Bayan Obo aeschynite.

	Aeschynite in fluorite-rich REE-Fe ores (n = 28)			Aeschynite in sodium-amphibole-rich REE-Fe ores (n = 18)			Aeschynite in aegirine-rich REE-Fe ores (n = 12)			Aes in slightly-altered ore-hosting dolomite (n = 8)			Aeschynite in vein-type of ores or veinlets (n = 45)		
	min	max	ave	min	max	ave	min	max	ave	min	max	ave	min	max	ave
TiO_2	20.35	34.31	26.76	17.98	28.02	23.59	22.48	28.58	26.12	19.96	23.61	21.72	16.73	32.31	25.24
Nb_2O_5	16.29	35.33	24.36	23.19	37.97	30.34	21.61	28.60	24.93	25.65	40.09	35.23	20.44	39.71	29.34
Ta_2O_5	0.01	0.01	0.01	0.02	0.23	0.14	0.08	0.16	0.12	0.11	0.21	0.17	0.03	0.16	0.08
Fe_2O_3	0.49	1.78	0.91	0.63	1.74	1.02	0.51	3.99	2.87	0.31	3.43	1.05	0.31	2.33	0.82
MgO	0.01	0.06	0.02	u.d.	0.57	0.08	0.01	0.07	0.03	u.d.	0.08	0.02	u.d.	0.16	0.04
Al_2O_3	u.d.	0.12	0.04	0.01	0.02	0.02	u.d.	0.02	0.01	u.d.	0.05	0.02	0.01	0.12	0.04
SiO_2	u.d.	2.09	0.54	0.01	1.72	0.26	0.03	4.76	3.18	1.75	2.28	2.02	u.d.	3.53	0.62
CaO	0.71	1.51	1.06	0.90	2.35	1.51	1.48	3.32	2.61	2.63	3.88	3.32	0.58	3.19	1.40
MnO	0.02	0.06	0.04	u.d.	u.d.	u.d.	0.04	0.34	0.19	0.31	0.34	0.33	u.d.	u.d.	u.d.
SrO	u.d.	0.06	0.02	0.01	0.01	0.01	0.01	0.01	0.01	0.01	0.10	0.04	u.d.	0.16	0.05
Y_2O_3	0.26	2.71	0.74	0.29	0.76	0.47	0.43	5.87	4.09	0.36	1.02	0.59	0.39	1.86	0.90
ZrO_2	0.01	0.04	0.02	0.01	0.08	0.04	0.01	0.02	0.01	u.d.	u.d.	u.d.	u.d.	0.05	0.02
BaO	0.02	3.02	0.73	0.03	0.26	0.11	0.19	0.42	0.26	0.01	0.18	0.09	0.01	0.25	0.11
La_2O_3	0.06	1.59	0.69	0.07	2.64	0.58	0.02	4.36	1.19	1.57	4.05	3.29	0.03	2.71	0.66
Ce_2O_3	4.94	17.21	11.08	9.02	20.18	11.97	3.25	23.50	9.52	15.10	18.63	17.31	7.12	15.44	10.02
Pr_2O_3	0.39	1.93	1.15	0.64	2.04	1.27	0.22	1.85	0.71	1.18	1.83	1.55	0.48	1.65	0.86
Nd_2O_3	11.86	22.60	16.35	13.14	19.71	17.88	2.96	9.58	6.17	8.40	9.80	8.85	6.57	19.91	16.64
Sm_2O_3	1.98	4.98	3.55	0.59	4.34	3.18	1.24	2.60	1.92	1.29	3.55	1.93	1.17	6.81	4.05
Eu_2O_3	1.01	2.15	1.66	0.92	1.80	1.49	0.65	1.31	1.03	0.84	1.38	1.00	0.69	2.25	1.67
Gd_2O_3	0.33	2.04	1.14	0.21	1.40	0.86	0.19	2.59	1.77	0.78	1.31	0.94	0.70	2.15	1.40
Dy_2O_3	0.08	1.76	0.55	0.10	0.55	0.33	0.14	5.34	3.27	0.40	1.47	0.67	0.13	1.13	0.59
Ho_2O_3	0.03	0.43	0.18	0.01	0.51	0.16	0.07	0.95	0.57	0.08	0.15	0.11	0.01	0.65	0.21
ThO_2	1.05	19.83	8.01	0.63	9.23	5.11	0.32	3.66	2.04	0.09	0.78	0.27	0.20	11.65	4.95
UO_2	0.02	0.12	0.06	0.01	0.01	0.01	0.01	0.14	0.07	u.d.	0.13	0.05	0.01	0.11	0.04
F	0.03	0.37	0.21	0.01	0.33	0.13	0.03	0.45	0.21	0.09	0.41	0.25	0.01	0.31	0.11
Total	94.69	101.54	99.11	98.53	101.41	100.01	87.48	99.45	92.52	94.34	101.17	98.85	81.93	101.87	99.20
							Calculate in 6(O + F)								
ΣB	1.91	2.09	2.01	1.91	2.04	2.01	1.98	2.05	2.01	1.98	2.01	2.00	1.97	2.08	2.04
Ti	0.95	1.56	1.27	0.85	1.34	1.11	1.05	1.29	1.19	0.90	1.10	0.99	0.86	1.49	1.17
Nb	0.49	0.99	0.69	0.67	1.08	0.86	0.59	0.80	0.69	0.72	1.09	0.96	0.57	1.09	0.82
Ta	< 0.005	< 0.005	< 0.005	< 0.005	< 0.005	< 0.005	< 0.005	< 0.005	< 0.005	< 0.005	< 0.005	< 0.005	< 0.005	< 0.005	< 0.005
Fe3 +	0.02	0.08	0.04	0.03	0.08	0.05	0.02	0.18	0.13	0.01	0.16	0.05	0.01	0.12	0.04
ΣA	1.00	1.22	1.07	1.01	1.14	1.04	1.05	1.14	1.10	1.01	1.19	1.06	0.98	1.06	1.01
Mg	< 0.005	0.01	< 0.005	u.d.	0.05	< 0.005	< 0.005	0.01	< 0.005	u.d.	0.01	< 0.005	u.d.	0.02	< 0.005
Al	u.d.	0.01	< 0.005	< 0.005	< 0.005	< 0.005	u.d.	< 0.005	< 0.005	u.d.	< 0.005	< 0.005	< 0.005	0.01	< 0.005
Si	u.d.	0.13	0.02	< 0.005	0.11	0.01	< 0.005	0.29	0.19	< 0.005	0.14	0.03	u.d.	0.24	0.02
Ca	0.05	0.10	0.07	0.06	0.16	0.10	0.10	0.22	0.17	0.18	0.25	0.22	0.04	0.22	0.09
Mn	< 0.005	< 0.005	< 0.005	u.d.	u.d.	u.d.	< 0.005	0.02	0.01	< 0.005	0.02	< 0.005	u.d.	u.d.	u.d.
Sr	u.d.	< 0.005	< 0.005	< 0.005	< 0.005	< 0.005	< 0.005	< 0.005	< 0.005	< 0.005	< 0.005	< 0.005	u.d.	0.01	< 0.005
Y	0.01	0.09	0.02	0.01	0.03	0.02	0.01	0.19	0.13	0.01	0.03	0.02	0.01	0.06	0.03
Zr	< 0.005	< 0.005	< 0.005	< 0.005	< 0.005	< 0.005	< 0.005	< 0.005	< 0.005	u.d.	u.d.	u.d.	u.d.	< 0.005	< 0.005
Ba	< 0.005	0.08	0.02	< 0.005	0.01	< 0.005	< 0.005	0.01	0.01	< 0.005	< 0.005	< 0.005	< 0.005	0.01	< 0.005
La	< 0.005	0.04	0.01	< 0.005	0.06	0.01	< 0.005	0.10	0.02	0.04	0.09	0.07	< 0.005	0.06	0.02
Ce	0.11	0.38	0.25	0.21	0.45	0.27	0.07	0.53	0.21	0.34	0.41	0.38	0.16	0.34	0.23
Pr	0.01	0.04	0.03	0.01	0.05	0.03	< 0.005	0.04	0.02	0.03	0.04	0.03	0.01	0.04	0.02
Nd	0.26	0.51	0.37	0.29	0.44	0.40	0.07	0.21	0.13	0.18	0.22	0.19	0.16	0.44	0.37
Sm	0.04	0.11	0.08	0.01	0.09	0.07	0.03	0.06	0.04	0.03	0.08	0.04	0.03	0.14	0.09
Eu	0.02	0.05	0.04	0.02	0.04	0.03	0.01	0.03	0.02	0.02	0.03	0.02	0.02	0.05	0.04
Gd	0.01	0.05	0.02	< 0.005	0.03	0.02	< 0.005	0.05	0.04	0.02	0.03	0.02	0.02	0.04	0.03
Dy	< 0.005	0.03	0.01	< 0.005	0.01	0.01	< 0.005	0.11	0.06	0.01	0.03	0.01	< 0.005	0.02	0.01
Ho	< 0.005	0.01	< 0.005	< 0.005	0.01	< 0.005	< 0.005	0.02	0.01	< 0.005	< 0.005	< 0.005	< 0.005	0.01	< 0.005
Th	0.01	0.29	0.12	0.01	0.13	0.07	< 0.005	0.05	0.03	< 0.005	0.01	< 0.005	< 0.005	0.16	0.07
U	< 0.005	< 0.005	< 0.005	< 0.005	< 0.005	< 0.005	< 0.005	< 0.005	< 0.005	u.d.	< 0.005	< 0.005	< 0.005	< 0.005	< 0.005
F	< 0.005	0.08	0.03	< 0.005	0.06	0.02	< 0.005	0.09	0.04	0.02	0.08	0.05	< 0.005	0.06	0.01

Meanwhile, fersmite contains Nb/Ta ratios (14.3–36.4, ave, 24.4) lower than other Nb-bearing minerals but generally comparable to or slightly higher than mantle values (17.39 for PM in Sun and McDonough (1989)), because fersmite contains extremely high Ta composition (9772–29,837 ppm). Ilmenorutile associated with aeschynite (17BY04) presents higher Nb/Ta ratios (36,853–47,122) than ilmenorutile from other samples (62.6–3098).

Monominerals of aeschynite megacrysts from seven samples have been picked out from diverse ores or ore-hosting dolomite and were then dissolved. Trace elements were analyzed to obtain accurate composition of HREE, Ta, Rb, Sr, Sm and Nd (Table 8). The content of Rb, Sr, Sm and Nd were measured for the following isotopic analyses. The REE content measured by ICP-MS was slightly over half of the values obtained by LA-ICPMS, indicating aeschynite in the monomineral samples were not completely separated from associated REE- and Nb-depleted minerals, and monazite or fluorocarbonate, which contain much higher ΣREE than aeschynite were unlikely to be comprised in the seven monomineral collections. The Y/Ho ratios of these aeschynite megacrysts display in a range of 14.2–21.0. Meanwhile, Ta is rather rare in these aeschynite with Nb/Ta ratios of 370.0 for 19BY04 and 973.8–9469.2 for the rest of samples.

5.3. Rb-Sr, Sm-Nd isotopic components of aeschynite megacrysts

The Rb-Sr and Sm-Nd isotopic ratios of the seven aeschynite dissolution have been measured (Table 9). These megacrysts of aeschynite

Table 2
Major element composition of Bayan Obo ilmenorutile.

	17BY04-n2	17BY04-1		17BY197-n4b	17BY197-n4d		17BY197-1				15BY99-1				
TiO_2	45.54	45.12	45.90	76.14	87.96	84.39	89.41	85.21	89.42	79.20	94.47	94.54	96.72	95.05	93.68
Nb_2O_5	28.48	29.51	30.19	15.31	7.47	9.06	6.39	8.89	6.05	12.07	3.21	3.06	2.15	3.26	3.56
Ta_2O_5	u.d.	u.d.	u.d.	0.13	0.12	u.d.	0.19	0.02	0.07	u.d.	u.d.	0.31	u.d.	0.25	0.01
MgO	0.16	0.13	0.20	0.02	u.d.	0.01	0.02	0.01	u.d.	u.d.	u.d.	0.02	u.d.	u.d.	u.d.
Al_2O_3	0.13	0.11	0.11	u.d.	u.d.	0.01	u.d.	0.00	0.00	u.d.	u.d.	u.d.	0.02	0.01	0.01
CaO	1.20	0.85	0.83	u.d.	0.01	0.01	0.03	0.02	0.03	0.01	0.29	0.29	0.45	0.28	0.59
MnO	0.11	0.18	0.11	0.01	u.d.	u.d.	0.01	u.d.	0.01	u.d.	0.01	0.02	u.d.	0.02	0.01
FeO	10.27	11.65	11.62	8.07	4.48	5.30	3.84	5.22	3.88	7.11	1.59	1.51	1.13	1.61	1.73
SrO	u.d.	0.02	u.d.	u.d.	u.d.	u.d.	0.02	0.02	u.d.	0.01	u.d.	u.d.	u.d.	u.d.	u.d.
Y_2O_3	0.16	0.04	0.03	0.01	0.04	0.02	u.d.	0.02	u.d.	0.01	0.01	0.02	u.d.	0.01	0.04
ZrO_2	0.04	u.d.	0.06	u.d.	u.d.	0.04	u.d.	0.05	u.d.	0.01	0.26	0.21	0.06	0.16	0.20
BaO	0.44	0.47	0.58	0.21	0.26	0.22	0.25	0.15	0.15	0.30	0.30	0.35	0.10	0.20	0.35
PbO	0.20	0.21	0.23	0.04	0.02	0.00	u.d.	0.08	u.d.	0.08	0.10	0.03	0.01	0.02	u.d.
ThO_2	4.07	5.72	3.46	u.d.	0.01	u.d.	u.d.	u.d.	0.03	0.00	0.00	0.05	0.05	u.d.	0.00
UO_2	0.03	0.05	0.02	u.d.	0.01	u.d.	u.d.	u.d.	u.d.	u.d.	u.d.	u.d.	0.03	u.d.	u.d.
total	90.84	94.06	93.34	99.93	100.38	99.04	100.16	99.69	99.65	98.80	100.24	100.41	100.72	100.88	100.17
Calculate in 2O															
Ti	0.60	0.59	0.59	0.83	0.91	0.90	0.93	0.90	0.93	0.86	0.96	0.96	0.97	0.96	0.96
Nb	0.23	0.23	0.23	0.10	0.05	0.06	0.04	0.06	0.04	0.08	0.02	0.02	0.01	0.02	0.02
Ta	u.d.	u.d.	u.d.	< 0.005	< 0.005	u.d.	< 0.005	< 0.005	< 0.005	u.d.	u.d.	< 0.005	u.d.	< 0.005	< 0.005
Mg	< 0.005	< 0.005	0.01	< 0.005	u.d.	< 0.005	< 0.005	< 0.005	u.d.	u.d.	u.d.	< 0.005	u.d.	u.d.	u.d.
Al	< 0.005	< 0.005	< 0.005	u.d.	u.d.	< 0.005	u.d.	< 0.005	< 0.005	u.d.	u.d.	u.d.	< 0.005	< 0.005	< 0.005
Ca	0.02	0.02	0.02	u.d.	< 0.005	< 0.005	< 0.005	< 0.005	< 0.005	< 0.005	< 0.005	< 0.005	0.01	< 0.005	0.01
Mn	< 0.005	< 0.005	< 0.005	< 0.005	u.d.	u.d.	< 0.005	u.d.	< 0.005	u.d.	< 0.005	< 0.005	u.d.	< 0.005	< 0.005
Fe	0.15	0.17	0.17	0.10	0.05	0.06	0.04	0.06	0.04	0.09	0.02	0.02	0.01	0.02	0.02
Sr	u.d.	< 0.005	u.d.	u.d.	u.d.	u.d.	< 0.005	< 0.005	u.d.	< 0.005	u.d.	u.d.	u.d.	u.d.	u.d.
Y	< 0.005	< 0.005	< 0.005	< 0.005	< 0.005	< 0.005	u.d.	< 0.005	u.d.	< 0.005	< 0.005	< 0.005	u.d.	< 0.005	< 0.005
Zr	< 0.005	u.d.	< 0.005	u.d.	u.d.	< 0.005	u.d.	< 0.005	u.d.	< 0.005	< 0.005	< 0.005	< 0.005	< 0.005	< 0.005
Ba	< 0.005	< 0.005	< 0.005	< 0.005	< 0.005	< 0.005	< 0.005	< 0.005	< 0.005	< 0.005	< 0.005	< 0.005	< 0.005	< 0.005	< 0.005
Pb	< 0.005	< 0.005	< 0.005	< 0.005	< 0.005	< 0.005	u.d.	< 0.005	u.d.	< 0.005	< 0.005	< 0.005	< 0.005	< 0.005	< 0.005
Th	0.02	0.02	0.01	u.d.	< 0.005	u.d.	u.d.	u.d.	< 0.005	< 0.005	< 0.005	< 0.005	< 0.005	u.d.	< 0.005
U	< 0.005	< 0.005	< 0.005	u.d.	< 0.005	u.d.	u.d.	u.d.	u.d.	u.d.	u.d.	u.d.	< 0.005	u.d.	u.d.

Table 3
Major element composition of Bayan Obo fersmite.

	06B283 (n = 7)			05B184	
	min	max	ave		
TiO_2	u.d.	0.02	0.01	3.21	3.37
Nb_2O_5	76.04	78.26	77.08	62.52	63.93
Ta_2O_5	1.22	2.36	1.87	0.10	0.19
Na_2O	u.d.	u.d.	u.d.	5.85	5.93
MgO	0.11	0.33	0.18	0.04	0.04
Al_2O_3	u.d.	0.03	0.03	0.04	0.02
SiO_2	u.d.	0.05	0.04	0.09	0.02
CaO	15.57	16.59	16.28	15.55	15.55
Fe_2O_3	0.27	0.94	0.60	0.46	0.55
MnO	0.18	0.24	0.20	0.04	0.05
SrO	u.d.	u.d.	u.d.	0.37	0.33
Y_2O_3	0.09	0.21	0.14	0.03	0.03
ZrO_2	u.d.	0.08	0.05	u.d.	0.00
BaO	u.d.	0.10	0.05	0.08	0.10
La_2O_3	0.05	0.43	0.27	0.09	0.07
Ce_2O_3	0.82	1.91	1.14	1.08	1.11
Pr_2O_3	0.07	0.18	0.13	0.06	0.10
Nd_2O_3	0.24	0.92	0.55	0.68	0.69
Sm_2O_3	u.d.	0.21	0.11	0.02	0.05
Eu_2O_3	u.d.	0.16	0.08	0.02	0.13
Gd_2O_3	u.d.	0.22	0.14	u.d.	0.05
Dy_2O_3	u.d.	0.21	0.15	0.06	u.d.
Ho_2O_3	u.d.	0.21	0.14	0.03	0.40
ThO_2	u.d.	0.05	0.01	0.56	0.66
UO_2	u.d.	0.02	0.01	u.d.	u.d.
F	u.d.	u.d.	u.d.	5.18	5.53
Total	98.21	99.74	98.99	96.13	98.90
		Calculate in 6(O + F)			
ΣB	1.96	1.99	1.98	1.59	1.59
Ti	u.d.	0.00	0.00	0.12	0.13
Nb	1.91	1.94	1.93	1.45	1.44
Ta	0.02	0.04	0.03	0.00	0.00
Fe3+	0.01	0.04	0.02	0.02	0.02
ΣA	1.03	1.07	1.05	1.51	1.48
Na	u.d.	u.d.	u.d.	0.58	0.57
Mg	0.01	0.03	0.01	0.00	0.00
Al	u.d.	0.00	0.00	0.00	0.00
Si	u.d.	0.00	0.00	0.00	0.00
Ca	0.93	0.98	0.97	0.86	0.83
Mn	0.01	0.01	0.01	0.00	0.00
Sr	u.d.	u.d.	u.d.	0.01	0.01
Y	0.00	0.01	0.00	0.00	0.00
Zr	u.d.	0.00	0.00	u.d.	0.00
Ba	u.d.	0.00	0.00	0.00	0.00
La	0.00	0.01	0.01	0.00	0.00
Ce	0.02	0.04	0.02	0.02	0.02
Pr	0.00	0.00	0.00	0.00	0.00
Nd	0.00	0.02	0.01	0.01	0.01
Sm	u.d.	0.00	0.00	0.00	0.00
Eu	u.d.	0.00	0.00	0.00	0.00
Gd	u.d.	0.00	0.00	u.d.	0.00
Dy	u.d.	0.00	0.00	0.00	0.00
Ho	u.d.	0.00	0.00	0.00	0.01
Th	u.d.	0.00	0.00	0.01	0.01
U	u.d.	0.00	0.00	u.d.	u.d.
F	u.d.	u.d.	u.d.	0.84	0.87

present radiogenic Sr isotopic composition, with $^{87}Sr/^{86}Sr$ varying in the range of 0.705921 ± 0.000011 to 0.706381 ± 0.000010. The $^{87}Rb/^{86}Sr$ ratios of all samples are below 0.23 (0.010–0.225). As for the $^{147}Sm/^{144}Nd$ ratios, all samples gave values between 0.11 and 0.16. And the $^{143}Nd/^{144}Nd$ ratios of these aeschynite solution are scattered between 0.511642 ± 0.000008 and 0.512762 ± 0.000008.

6. Discussion

6.1. Hydrothermal origin of Nb-bearing minerals

Aeschynite-associated minerals generally have hydrothermal origins. For example, the fluoritization has been demonstrated occurred during two hydrothermal metasomatism events, a Mesoproterozoic one triggered by carbonatite intrusion and a Paleozoic one subjected to subduction of Paleo-Asian oceanic crust (Liu et al., 2018b), corresponding to two REE mineralization events. Meanwhile, the alkali silicates (e.g. aegirine, Na-amphibole, and phlogopite) within the ore-hosting dolomite were product of typical carbonatite-related hydrothermal alteration (Liu et al., 2018a; Wang et al., 2019). Disseminated and massive magnetite aggregates in the ore-hosting dolomite have similar trace element characteristics to hydrothermal magnetite in skarn Fe deposits (Huang et al., 2015). Besides, mica slabs and pyrite megacrysts in the typical vein-type of ores have Paleozoic Rb-Sr (459 ± 41 Ma or 309 ± 12 Ma) and Re-Os isochron ages (439 ± 86 Ma), respectively (Liu et al., 2004; Hu et al., 2009; Yang et al., 2007), therefore regarded as characteristic Paleozoic gangue minerals. On the contrary, some minerals in the ore-hosting dolomite have explicit Mesoproterozoic primary origin, such as the coarse-grained dolomite and apatite with Sm-Nd isochron age of 1341 ± 160 Ma and 1317 ± 140 Ma (Chen et al., 2019; Hu et al., 2019; Yang et al., 2019; Liu et al., 2020). All above minerals would help to form the paragenesis of Nb-bearing minerals.

Based on petrographic observation, aeschynites in the fluorite-rich or Na-amphibole-rich ores (Group 1) are generally fine-grained and interstitial to magnetite grains, replacing massive sodium-amphiboles, fluorite as well as micas. And a few euhedral aeschynite megacrysts (also Group 1) in the vein-type of ores are associated with barite and sulfide (Liu et al., 2004). Therefore, the aeschynite of Group 1 has apparent Paleozoic hydrothermal origin. However, aeschynite of Group 2 (Aes. in aegirine-rich ores) is corroded by apatite, a kind of primary gangue mineral with multiphase hydrothermal overprints (Hu et al., 2019; Ren et al., 2019; Yang et al., 2019). Meanwhile, aeschynites of Group 3 in the slightly-altered ore-hosting dolomite are directionally aligned and associated with fluorite and iron oxides. In summary, a hydrothermal origin was supported for aeschynite of Group 1 and 3 according to petrography, while determining the origin of aeschynite of Group 2 needs further geochemical evidence. Besides, considering there is no associated Paleozoic gangue minerals, aeschynite of Group 2 (except 19BY04) and 3 were formed during the Mesoproterozoic carbonatite-related magmatic-hydrothermal processes.

Ilmenorutiles are associated with Paleozoic hydrothermal minerals, micas and sulfide, crystallized as interstitial grains among massive magnetite aggregates, or enclaved aeschynite fragments, indicating a Paleozoic hydrothermal origin.

'Wormlike' fersmites are associated with or replaced by anhedral magnetite in the slightly-altered ore-hosting dolomite (both coarse- and fine-grained ore-hosting dolomite). The coarse-grained dolomite has been proved to be primary in origin (Chen et al., 2019; Liu et al., 2020), and fersmite observed in this study is likely to have an igneous origin. Interstitial anhedral columbite in the aegirine-rich and apatite-rich ores are closely associated with barite, massive or banded magnetite aggregates. A Paleozoic hydrothermal origin was suggested for these columbite grains. Even though euhedral primary columbites have been reported in local calciocarbonatite dykes (Le Bas et al., 1992), columbite in the open pits presents distinct petrographic characteristics. Besides, in the observed carbonatite dykes, columbite is too rare to support extensive Nb mineralization from the carbonatite melt. Anhedral baotite was formed postdating the Mesoproterozoic massive iron oxides with no associated Paleozoic gangue minerals. While fergusonite replaced fluorite vein and micas slabs, indicating its Paleozoic hydrothermal origin.

Based on geochemical characteristics, analyzed aeschynite,

Table 4
Major element composition of Bayan Obo columbite.

	Columbite-(Mn)17BY196 (n = 8)			Columbite-(Fe)05B184 (n = 4)			Columbite-(Mg)06B283 (n = 7)		
	min	max	ave	min	max	ave	min	max	ave
TiO_2	0.23	0.32	0.26	1.97	2.23	2.06	u.d.	0.04	0.03
Nb_2O_5	73.00	75.98	74.93	72.93	75.55	74.67	77.23	79.85	78.57
Ta_2O_5	u.d.	0.08	0.04	u.d.	0.03	0.03	1.41	2.71	2.07
MgO	0.04	0.08	0.06	0.31	0.36	0.33	6.14	6.77	6.53
SiO_2	u.d.	0.02	0.01	u.d.	u.d.	u.d.	0.02	0.11	0.06
CaO	0.13	0.37	0.29	0.03	0.06	0.04	0.12	0.17	0.14
MnO	17.56	18.21	18.00	3.32	4.48	4.14	2.04	2.62	2.36
FeO	4.19	5.33	4.72	17.43	18.66	17.89	7.71	8.79	8.18
Y_2O_3	0.22	0.66	0.52	0.08	0.10	0.09	0.05	0.13	0.07
ZrO_2	u.d.	u.d.	u.d.	u.d.	0.03	0.03	0.02	0.24	0.10
BaO	u.d.	0.08	0.05	0.01	0.10	0.06	u.d.	0.17	0.07
PbO	0.26	0.39	0.31	0.23	0.34	0.28	0.30	0.39	0.34
ThO_2	u.d.	0.07	0.03	u.d.	0.05	0.05	u.d.	0.03	0.02
UO_2	u.d.	0.03	0.02	u.d.	0.05	0.05	u.d.	0.04	0.02
Total	97.32	100.78	99.18	98.01	100.30	99.61	96.83	100.21	98.48
				Calculate in 6O					
ΣB	1.93	1.96	1.94	1.98	1.99	1.99	1.97	1.98	1.98
Ti	0.01	0.01	0.01	0.08	0.10	0.09	u.d.	0.00	0.00
Nb	1.92	1.95	1.93	1.89	1.91	1.90	1.94	1.96	1.95
Ta	u.d.	0.00	0.00	u.d.	0.00	0.00	0.02	0.04	0.03
ΣA	1.10	1.17	1.14	1.06	1.09	1.08	1.03	1.06	1.05
Mg	0.00	0.01	0.00	0.03	0.03	0.03	0.52	0.55	0.54
Si	u.d.	0.00	0.00	u.d.	u.d.	u.d.	0.00	0.01	0.00
Ca	0.01	0.02	0.02	0.00	0.00	0.00	0.01	0.01	0.01
Mn	0.84	0.90	0.87	0.16	0.21	0.20	0.09	0.12	0.11
Fe2+	0.20	0.25	0.22	0.81	0.89	0.84	0.35	0.41	0.37
Y	0.01	0.02	0.02	0.00	0.00	0.00	0.00	0.00	0.00
Zr	u.d.	u.d.	u.d.	u.d.	0.00	0.00	0.00	0.01	0.00
Ba	u.d.	0.00	0.00	0.00	0.00	0.00	u.d.	0.00	0.00
Pb	0.00	0.01	0.00	0.00	0.01	0.00	0.00	0.01	0.01
Th	u.d.	0.00	0.00	u.d.	0.00	0.00	u.d.	0.00	0.00
U	u.d.	0.00	0.00	u.d.	0.00	0.00	u.d.	0.00	0.00

Table 5
Major element composition of Bayan Obo baotite.

	17BY06-1			17BY06-2			17BY10-1			
SiO_2	14.25	14.31	14.12	14.41	13.90	14.41	14.12	14.84	14.27	14.41
TiO_2	23.94	23.97	23.26	24.54	20.17	24.00	27.76	27.81	24.66	25.51
FeO	5.11	5.65	5.74	5.57	6.76	5.91	3.65	3.82	4.89	4.70
Nb_2O_5	16.37	16.46	16.56	16.30	19.51	16.52	13.32	13.09	15.34	15.12
MgO	u.d.	u.d.	u.d.	u.d.	u.d.	0.01	u.d.	0.01	u.d.	u.d.
Al_2O_3	u.d.	0.04	0.02	0.03	u.d.	0.03	0.01	0.02	u.d.	0.00
CaO	0.02	0.00	u.d.	u.d.	0.01	u.d.	0.05	0.03	0.01	0.05
MnO	0.02	u.d.	0.03	0.03	0.01	0.01	0.01	0.04	0.03	0.04
SrO	0.27	0.19	0.24	0.36	0.15	0.35	0.07	0.01	0.14	0.22
BaO	38.57	37.67	37.86	38.53	38.38	38.61	40.31	38.69	38.41	39.48
Cl	2.25	2.31	2.28	2.29	2.23	2.30	1.79	2.18	2.16	2.18
Total	100.81	100.62	100.11	102.06	101.13	102.14	101.09	100.54	99.89	101.70
Calculate in 24O										
Si	3.90	3.90	3.89	3.88	3.86	3.89	3.81	3.97	3.91	3.89
ΣB	8.09	8.20	8.18	8.18	8.21	8.20	8.05	8.01	8.09	8.06
Ti	4.91	4.90	4.81	4.95	4.20	4.86	5.61	5.58	5.07	5.16
Fe2+	1.16	1.28	1.32	1.25	1.56	1.33	0.82	0.85	1.12	1.06
Nb	2.02	2.02	2.06	1.98	2.44	2.01	1.62	1.58	1.90	1.84
ΣA	4.19	4.07	4.14	4.14	4.21	4.15	4.29	4.09	4.16	4.24
Mg	u.d.	u.d.	u.d.	u.d.	u.d.	< 0.005	u.d.	< 0.005	u.d.	u.d.
Al	u.d.	0.01	0.01	0.01	u.d.	0.01	< 0.005	0.01	u.d.	< 0.005
Ca	0.01	< 0.005	u.d.	u.d.	< 0.005	u.d.	0.01	0.01	< 0.005	0.01
Mn	0.01	u.d.	0.01	0.01	< 0.005	< 0.005	< 0.005	0.01	0.01	0.01
Sr	0.04	0.03	0.04	0.06	0.02	0.05	0.01	< 0.005	0.02	0.03
Ba	4.13	4.02	4.09	4.07	4.18	4.09	4.26	4.06	4.13	4.18
Cl	1.04	1.06	1.06	1.04	1.05	1.05	0.81	0.99	1.00	0.99

ilmenorutile and fersmite contain Y/Ho ratios consistently lower than values of chondrite or primitive mantle, while the Y/Ho ratios of baotite are much higher than mantle values (Fig. 10.). Carbonatite and the unaltered coarse-grained ore-hosting dolomite keep the chondritic ratios (Liu et al., 2020). While in an aqueous system, the Y/Ho ratios would be either elevated as in seawater or hydrothermal fluorite, or decreased as in hydrothermal carbonates, both deviating from the chondritic value anyway and varying in a large range (Bau, 1996).

Table 6
Major element composition of Bayan Obo fergusonite.

	14BY3-4 dark (n = 8)			14BY3-4 bright (n = 5)		
	min	max	ave	min	max	ave
Nb_2O_5	45.27	47.35	46.43	42.02	43.44	42.67
TiO_2	0.04	0.23	0.14	0.18	0.45	0.30
MgO	u.d.	u.d.	u.d.	0.01	0.06	0.04
SiO_2	u.d.	0.02	0.01	1.78	2.88	2.54
CaO	0.06	0.25	0.13	1.04	1.43	1.25
FeO	0.06	0.25	0.15	1.10	2.01	1.70
MnO	u.d.	0.11	0.04	0.44	1.11	0.78
SrO	u.d.	0.04	0.04	0.02	0.04	0.03
Y_2O_3	20.18	21.44	20.75	11.98	16.31	13.44
La_2O_3	u.d.	0.08	0.05	0.04	0.10	0.06
Ce_2O_3	0.13	0.34	0.25	0.39	0.93	0.63
Pr_2O_3	u.d.	0.06	0.03	0.02	0.08	0.05
Nd_2O_3	0.78	1.60	1.12	1.31	2.65	1.91
Sm_2O_3	1.24	1.93	1.59	1.84	2.94	2.49
Eu_2O_3	0.62	1.25	0.87	1.06	1.82	1.54
Gd_2O_3	5.79	6.80	6.48	5.11	6.28	5.89
Tb_2O_3	0.76	0.99	0.85	0.65	1.16	0.96
Dy_2O_3	9.02	9.97	9.44	7.37	8.58	7.95
Ho_2O_3	2.26	3.09	2.67	0.92	1.70	1.31
Er_2O_3	2.62	3.84	3.33	0.87	1.97	1.30
Tm_2O_3	0.62	1.30	0.86	0.77	0.94	0.84
Yb_2O_3	0.89	1.89	1.47	0.11	0.72	0.37
Lu_2O_3	2.22	2.54	2.34	0.38	1.84	1.01
ThO_2	0.24	0.70	0.44	2.37	3.66	3.19
UO_2	0.01	0.05	0.03	0.00	0.08	0.04
F	u.d.	0.07	0.06	0.25	0.40	0.33
total	97.99	100.42	99.44	90.05	94.80	92.43
Calculate in 4(O + F)						
ΣB	0.99	1.00	0.99	0.92	0.96	0.94
Nb	0.98	1.00	0.99	0.91	0.94	0.92
Ti	< 0.005	0.01	0.01	0.01	0.02	0.01
ΣA	1.00	1.03	1.02	1.09	1.16	1.13
Mg	u.d.	u.d.	u.d.	< 0.005	< 0.005	< 0.005
Si	u.d.	< 0.005	< 0.005	0.09	0.14	0.12
Ca	< 0.005	0.01	0.01	0.05	0.07	0.06
Fe	< 0.005	0.01	0.01	0.05	0.08	0.07
Mn	u.d.	< 0.005	< 0.005	0.02	0.04	0.03
Sr	u.d.	< 0.005	< 0.005	< 0.005	< 0.005	< 0.005
Y	0.51	0.54	0.52	0.31	0.43	0.34
La	u.d.	< 0.005	< 0.005	< 0.005	< 0.005	< 0.005
Ce	< 0.005	0.01	< 0.005	0.01	0.02	0.01
Pr	u.d.	< 0.005	< 0.005	< 0.005	< 0.005	< 0.005
Nd	0.01	0.03	0.02	0.02	0.05	0.03
Sm	0.02	0.03	0.03	0.03	0.05	0.04
Eu	0.01	0.02	0.01	0.02	0.03	0.03
Gd	0.09	0.11	0.10	0.08	0.10	0.09
Tb	0.01	0.02	0.01	0.01	0.02	0.02
Dy	0.14	0.15	0.14	0.12	0.13	0.12
Ho	0.03	0.05	0.04	0.01	0.03	0.02
Er	0.04	0.06	0.05	0.01	0.03	0.02
Tm	0.01	0.02	0.01	< 0.005	0.01	0.01
Yb	0.01	0.03	0.02	< 0.005	0.01	0.01
Lu	0.03	0.04	0.03	0.01	0.03	0.01
Th	< 0.005	0.01	< 0.005	0.03	0.04	0.03
U	< 0.005	< 0.005	< 0.005	< 0.005	< 0.005	< 0.005
F	u.d.	0.01	< 0.005	0.04	0.06	0.05

Aeschynites of Group 2 with annulus, although replaced by apatite in the aegirine-rich ores, present Y/Ho ratios lower than chondritic value, verifying their hydrothermal origin. However, fersmite exhibits Y/Ho and Nb/Ta ratios close to the mantle/chondritic values, verifying fersmite as the only kind of analyzed mineral with evident igneous origin (columbite and fergusonite excluded, lack of data).

Based on Sr-Nd isotopic components, if calculated at the same age, aeschynite megacrysts are characterized by initial $^{87}Sr/^{86}Sr$ ratios intermediate between the values of carbonatite/ore-hosting dolomite and Permian granitoids (Fig. 13d). It is suggested that the radiogenic Sr components were introduced through crustal-contaminated hydrothermal fluids, instead of carbonatite-related magma or hydrothermal fluids.

In summary of petrographic, geochemical and isotopic evidence, we propose that the formation of aeschynite (both the Mesoproterozoic and the Paleozoic), ilmenorutile, baotite, columbite and fergusonite in the slightly-altered ore-hosting dolomite and different types of ores are attributed to hydrothermal Nb mineralization (Fig. 7). Aeschynite of Group 1 was formed in the Paleozoic hydrothermal fluids, and the Group 2 and 3 were formed in the Mesoproterozoic carbonatite-derived hydrothermal fluids. Fersmite in the slightly-altered ore-hosting dolomite likely have an igneous origin, similar to the euhedral columbites in calciocarbonatite dykes (Le Bas et al., 1992). Columbites in this study contain significantly variable major components but have consistent Paleozoic hydrothermal origin. Moreover, columbite has potential to record magmatic-hydrothermal evolution of the carbonatite, which deserves further detailed research. Baotite has a Mesoproterozoic hydrothermal origin. While ilmenorutile and fergusonite were formed at the Paleozoic. Considering aeschynite is the dominating Nb-bearing mineral in the East and Main open pits (Hou et al., 2018), a major hydrothermal origin of Nb mineralization in the Bayan Obo ore-hosting dolomite (East and Main Open Pits) was supported by this study.

6.2. Extreme Nb-Ta fractionation of Nb-bearing minerals

Analyzed aeschynites are extremely depleted in Ta (far below the detection limit of EMPA). It indicates that: (1) the precipitation of aeschynite accompanied significant Nb-Ta fractionation, or (2) the fluids had suffered Nb-Ta fractionation preceding the hydrothermal Nb mineralization. The former assumption is unlikely because both Nb and Ta are extremely rare in aeschynite-associated ore-forming minerals, e.g. fluorite, aegirine, sodium amphibole and dolomite (Liu et al., 2018a, 2018b; Chen et al., 2019). Moreover, different kinds of bulk ores (Nb/Ta: 76–1665, n = 640; IGCAS, 1988; Zhang et al., 2003), especially the high-grade ones suffered extensive fluorine-alkali metasomatism (Nb/Ta: 54–262, n = 219; IGCAS, 1988), whole rock of the ore-hosting dolomite (Nb/Ta: 152–5479, n = 18; Sun et al., 2014; Chen et al., 2019) and local carbonatite dykes (Nb/Ta: 14–82, n = 8; Yang et al., 2011a) all present higher Nb/Ta ratios than the average crust (11.4; Rudnick and Gao, 2003), primitive mantle (17.8; McDonough and Sun, 1995) and global carbonatite (34.9, n = 104; Chakhmouradian, 2006). The Bayan Obo carbonatite dykes have Nb/Ta ratios in the similar range as the bulk ores or the ore-hosting dolomite (Fig. 11). And the enclaved H9 slate layer in the ore-hosting dolomite (Fig. 2), which also suffered extensive alkaline alteration (Zhang et al., 1997; Xiao et al., 2012; Liu et al., 2018a), presents as variable Nb/Ta ratios as the carbonatite and ores (17.1–1769; Zhang et al., 2003). Therefore, it is more reasonable for the second hypothesis that the Nb-Ta fractionation occurred during the generation of carbonatite magma or related hydrothermal fluids, rather than fractional crystallization during the Nb mineralization process. The high Nb/Ta ratio is a geochemical feature inherited from the carbonatite-related magmatic-hydrothermal system.

The Bayan Obo carbonatite has been regarded as mantle-derived primary carbonatite according to the facts that: (1) there is no exposed or drilled associated alkali igneous rocks; (2) its composition evolves from dolomitic- to calcio-carbonatite, which is contradict to the evolution of high-fractionated carbonatite derived from the crust (Lee and Wyllie, 1998). The carbonated peridotite, especially carbonated lherzolite, has been experimentally demonstrated as a potential source of primary dolomitic carbonatite melt (Wallace and Green, 1998), and the low-degree melting of the $HFSE^{5+}$-enriched amphibole- or phlogopite-bearing lherzolite may play significant role in causing fractionation among HFSEs, especially causing higher Nb/Ta ratios of the fractional carbonatitic melt than the primitive mantle value (Chakhmouradian, 2006). The extreme Nb-Ta fractionation in Bayan Obo carbonatite and ores, therefore, is inherited as a primary geochemical characteristic of mantle-derived carbonatite. Hydrothermal Nb-bearing minerals in this

Table 7
In situ REE, other minor and trace element composition (ppm) of Nb oxides analyzed by LA-ICPMS.

	Aeschynite in fluorite-rich ores (n = 15)			Aeschynite in amphibole-rich ores (n = 7)			Aeschynite in aegirine-rich ores (n = 10)			Aeschynite in slightly-altered ore-hosting dolomite (n = 5)		
ppm	min	max	ave	min	max	ave	min	max	ave	min	max	ave
Y	6328	29,310	12,890	5877	11,470	8277	30,640	97,290	67,720	12,040	19,440	15,070
Nb	185,750	362,040	267,810	278,520	402,750	353,620	236,530	434,940	314,060	287,120	472,500	396,810
Ba	3.05	20,460	3916	2.10	2092	498.7	373.5	2525	1482	419.7	1209	767.6
La	3001	27,840	14,170	9238	48,330	20,430	10,720	63,260	29,320	12,410	62,840	38,730
Ce	72,380	205,020	152,430	132,260	273,780	187,260	63,060	255,010	134,070	148,180	236,300	193,880
Pr	16,010	53,110	39,570	40,740	58,950	49,420	13,380	36,950	22,080	24,350	34,300	30,090
Nd	65,610	286,300	223,180	294,280	350,270	323,980	61,550	146,900	100,130	120,700	150,760	136,770
Sm	10,750	66,080	43,530	46,430	62,120	54,940	20,670	33,840	26,140	24,630	39,120	29,930
Eu	3422	16,880	10,370	6824	12,590	9440	8175	12,250	9305	7160	12,110	8838
Gd	6492	26,960	16,280	8518	18,770	13,020	16,870	31,540	22,190	14,820	24,480	18,470
Tb	980.1	2888	1643	668.1	1675	1047	3129	9413	5749	2010	3768	2824
Dy	3908	11,320	6636	2513	6254	3860	16,950	61,640	39,980	8153	16,800	12,320
Ho	389.8	1837	852.3	316.5	810.5	527.5	2658	10,690	7222	842.8	1739	1295
Er	511.1	3664	1392	500.3	1397	909.7	4829	23,940	15,410	982.8	2358	1669
Tm	34.07	328.3	111.3	39.99	120.5	77.34	433.8	2654	1593	58.67	168.2	109.5
Yb	98.92	1160	361.3	138.7	471.8	293.0	1620	10,890	6216	163.5	563.4	340.9
Lu	5.75	84.45	23.69	8.38	37.26	20.71	124.8	783.0	493.1	9.53	37.82	21.64
Ta	4.55	99.7	39.79	2.80	8.98	5.68	109.6	331.3	181.2	114.9	219.5	158.0
Th	28,780	219,170	74,930	32,040	88,320	51,892	10,960	46,700	25,640	3185	37,560	16,760
U	10.19	207.7	54.69	4.92	66.98	37.15	425.0	2301	1234	146.2	1419	677.3
	Aeschynite megacrysts(n = 18)			Ilmenorutile(n = 11)			Baotite (n = 4)			**Fersmite(n = 6)**		
ppm	min	max	ave	min	max	ave	min	max	ave	min	max	ave
Y	8638	48,340	20,170	0.98	2815	742.7	3.54	4.66	3.96	86.32	834.2	445.1
Nb	234,810	401,040	317,320	18,260	256,790	123,590	62,660	79,340	71,340	278,170	513,300	417,850
Ba	0.82	3306	562.8	10.57	4015	984.0	189,810	217,420	207,860	4.04	1517.3	366.3
La	7407	36,740	13,770	4.16	2999	829.2	63.51	133.9	82.46	2704	11,870	5086
Ce	91,650	205,820	132,320	9.61	20,960	5588	35.15	72.16	50.29	5880	36,300	14,310
Pr	32,700	45,510	38,090	0.90	4088	1068	1.38	1.79	1.50	627.3	3699	1609
Nd	202,080	321,080	270,220	2.51	17,360	4404	1.77	2.09	1.95	2224	10,750	5167
Sm	40,610	90,510	66,640	0.41	3089	768.6	0.26	0.43	0.35	308.0	1198	704.6
Eu	8906	17,920	13,470	0.11	908.2	218.0	1.47	1.97	1.79	74.86	232.1	139.3
Gd	12,040	29,860	21,700	0.19	1835	464.6	134.3	152.4	147.7	123.3	676.3	339.5
Tb	988.8	3849	2219	0.04	332.9	78.17	0.01	0.07	0.03	14.06	76.37	38.57
Dy	3661	20,600	9386	0.34	1917	436.5	0.09	0.49	0.25	54.83	331.6	165.5
Ho	479.0	3531	1296	0.05	311.8	70.60	0.02	0.08	0.04	5.25	45.82	21.63
Er	863.9	6447	2183	0.17	641.3	145.7	0.01	0.15	0.09	7.90	82.56	39.84
Tm	78.29	459.4	169.9	0.01	67.69	15.40	0.00	0.01	0.01	0.78	8.00	3.91
Yb	318.1	1165	534.3	0.02	296.5	68.07	0.00	0.19	0.09	3.86	34.65	19.34
Lu	22.15	58.60	33.91	0.04	23.89	5.74	0.01	0.02	0.01	0.29	3.59	1.98
Ta	3.27	344.7	46.54	5.33	400.3	91.55	3.64	11.96	5.99	9772	29,840	19,380
Th	11,410	154,500	87,490	0.42	66,370	22,300	0.14	0.56	0.32	6.11	5312	958.7
U	97.87	2192	723.4	0.07	461.4	52.18	0.00	0.09	0.03	48.52	64,420	12,280

study are the prime carrier of Nb with extreme Nb/Ta ratios.

As comparison, during the magmatic-hydrothermal evolution of alkali granite, another common Nb-Ta host worldwide, the Nb/Ta ratios of granite-related Nb-bearing minerals decrease while Ta content increases, which seems contradicted to the hydrothermal origin of Bayan Obo Nb resources in the open pits (Zhu et al., 2015; Wu et al., 2018; Xie et al., 2018). However, there are several significant but ignored facts. (1) Global carbonatite melt (Nb/Ta: 25–39; Ta: 12–18 ppm) is characterized by far higher Nb/Ta ratios and less Ta than alkali granite melt (Nb/Ta: mostly < 10; Ta: mostly 10–200 ppm), especially the Bayan Obo carbonatite (Nb/Ta: 21–86; Ta: mostly < 1.8 ppm) (Table S7a). (2) Extreme depletion of Ta in Bayan Obo carbonatite makes Ta enrichment in subsequent hydrothermal process more difficult than Nb. The Bayan Obo Nb-bearing minerals contain Ta (max 2.7 ppm) much less than granite-related minerals (0.7–63.3; mostly > 2 ppm) (Table S7b). (3) The least Nb/Ta ratio of the major Bayan Obo Nb-bearing mineral (~25) is higher than the value of most granite-related Nb-bearing minerals (< 24) (Table S7b). Due to the general high Nb/Ta ratio and low Ta content of Bayan Obo carbonatite, the mass balance would be met if only small amount of low Nb/Ta (~8.5 as some ilmenorutile) Nb-bearing mineral fractionated from the hydrothermal fluids, while the rest of minerals still have rather high Nb/Ta ratios. (4) The Bayan Obo carbonatite dykes generally contain lower Nb and Ta than the recrystallized fine-grained ore-hosting dolomite (Table S7a), and the heterogeneous Nb distribution in the ore-hosting dolomite indicates significant involvement of hydrothermal Nb enrichment. (5) The most common primary Nb-host worldwide, pyrochlore, is extremely Nb-enriched and Ta-depleted. Theoretically, its extensive precipitation would cause extreme Nb-Ta fractionation in the residual melt and related hydrothermal fluids. However, the limited Nb-Ta content in Bayan Obo carbonatite demonstrates that the Nb-Ta fractionation caused by primary minerals is not prominent. (6) Nb-bearing minerals in this study have Nb/Ta ratios as variable as alkali granite-related hydrothermal ones (Table S7b). Therefore, the hydrothermal Nb-bearing minerals related to carbonatite are able to have high Nb/Ta ratios and high Nb content.

6.3. Relationship between REE and Nb mineralization

Although some Nb-bearing minerals are enriched in REEs, such as aeschynite and fergusonite, REE mineralization in Bayan Obo is represented by extensive precipitation of monazite and fluorocarbonates, which extremely lack of Nb. REE and Nb have long been regarded as cogenetic resources, both originated from carbonatite magma, transported through the same batches of melts or hydrothermal fluids and coprecipitated during the same metasomatic process (Smith and Spratt, 2012; Yang et al., 2017). As for direct source of REE and Nb, there is no other rocks that was able to provide as large amount of Nb and REE as in Bayan Obo deposit, except carbonatite. The rest of widespread rocks, including the Archean basement rock, the Mesoproterozoic metasedimentary rocks, as well as the Paleozoic granitoids-diorite, all contain disproportionate REE and Nb to the current reserves (Liu et al., 2011). However, in this study, it is proposed that the transportation and mineralization of REE and Nb present systematic difference. The Bayan Obo carbonatite, as magmatic host for both REE and Nb, is characterized by variable ΣREE and limited Nb composition (mostly < 250 ppm) (Le Bas et al., 1992; Tao et al., 1998; Wang et al., 2002; Yang et al., 2003; Fei, 2005; Yang et al., 2009, 2011; Lai et al., 2012; Ling et al., 2013). Meanwhile, the ore-hosting dolomite, which suffered slightly hydrothermal alteration, contains ΣREE in similar range of carbonatite, but much more variable Nb content, with half of the collected Nb content over 250 ppm (Fig. 12). In addition, extensively metasomatized ores have average Nb content (441 ppm − 986 ppm) higher than that of the ore-hosting dolomite (374 ppm) and the carbonatite (125 ppm). The above phenomenon indicates that REE would be enriched during both the magmatic and hydrothermal processes, while Nb enrichment in carbonatitic melt is limited. Alternatively, hydrothermal processes played more significant role in Nb enrichment.

Le Bas et al. (1992) used to recognize a few crystals of pyrochlore and ferrocolumbite in a local calciocarbonatite dyke, and defined their primary origin. There was barely other petrographic evidence of Nb-bearing minerals in other carbonatite dykes, which verifies our petrographic observation. The scarcity of Nb-bearing minerals conforms to the limited Nb composition in carbonatite dykes. In contrast, the hydrothermal Nb-bearing minerals, including aeschynite, columbite, ilmenorutile, fergusonite and baotite in this study, are more common hosts for Nb in the ore-hosting dolomite and high-grade ores. Besides, most of the hydrothermal Nb-bearing minerals have no closely associated fluorocarbonate or monazite, indicating the REE-Nb fractionation during their transport and deposition.

The aeschynites of Group 1 (Aeschynite-Nd), namely the Paleozoic aeschynite in the fluorite-rich ores, sodium-amphibole-rich ores and aeschynite megacrysts, are generally not associated with fluorocarbonate or monazite, and crystalized from REE-rich, relatively LREE-depleted and low-Ce/Nd fluids. These REE characteristics indicate a former fractionation of high-Ce/Nd REE minerals from the hydrothermal fluids. Bastnaesite and monazite in the ore-hosting dolomite are generally belong to the Ce-rich species and characterized by high Ce/Nd ratios (> 1.0) (IGCAS, 1988; Smith et al., 2000), playing as the major repository of Cerium. Thus it is very likely that the prominent Paleozoic REE mineralization occurred independently ahead of the formation of Group 1 aeschynite.

Moreover, the complex annulus (bright and dark annulus under BSE) of aeschynite-(Ce) in the aegirine-rich ores (Group 2) present variable REE patterns, relatively high Ce/Nd ratios for the bright annulus and opposite for the dark (Table S2), suggesting its precipitation accompanied repeatedly variable LREE composition in the hydrothermal fluids, which was controlled by precipitation of LREE-enriched minerals. Therefore, the Mesoproterozoic aeschynite in the aegirine-rich ores was formed nearly simultaneously to the Mesoproterozoic REE mineralization in the massive ores. As for small portion of Group 2 aeschynite (Paleozoic Aes. megacryst) that replaced REE minerals (19BY04), its high Ce/Nd ratio was caused by extraction of LREE (especially Ce) from earlier deposited REE minerals.

Nioboaeschynite (Group 3) presents higher Ce/Nd ratios, indicating that the precipitation of Mesoproterozoic aeschynite in the slightly-altered ore-hosting dolomite was not significantly influenced by REE mineralization. Since the carbonatite-derived fluids are LREE-enriched (Bühn and Rankin, 1999), the high-Ce/Nd aeschynite also suggests limited precipitation of Ce-rich monazite and fluorocarbonate in the ore-hosting dolomite, which is consistent with its lower ΣREE compared with diverse types of ores (Liu et al., 2020).

As primary Nb-bearing mineral, fersmite is characterized by LREE-rich patterns and high Ce/Nd ratio similar to calciocarbonatite dykes (Yang et al., 2011a), without hydrothermal extraction of LREE from the melt. Ilmenorutiles from different samples have significantly variable REE patterns. And the drastically variable ΣREE of ilmenorutiles was possibly caused by Ti-REE exchange in lattice. The most REE-enriched ilmenorutile has low Ce/Nd ratio, supporting an early LREE fractionation from the Paleozoic hydrothermal fluids. Fergusonite extremely lacks of LREE, and may precipitate postdating the extensive LREE fractionation from the Paleozoic hydrothermal fluids. Since baotite and columbite are REE-depleted accessory minerals and not associated with REE minerals in the ores, their REE characteristics have no essential relationship with REE mineralization.

In summary, the Bayan Obo Nb mineralization generally occurred postdating REE mineralization at the same stage, whereas high Ce/Nd ratios of the previously formed REE minerals might be occasionally inherited. As exception, aeschynite of Group 2 deposited simultaneously to the REE mineralization, however, spatially separated in the studied thin section.

The major Nb species in aqueous solution is still lack of

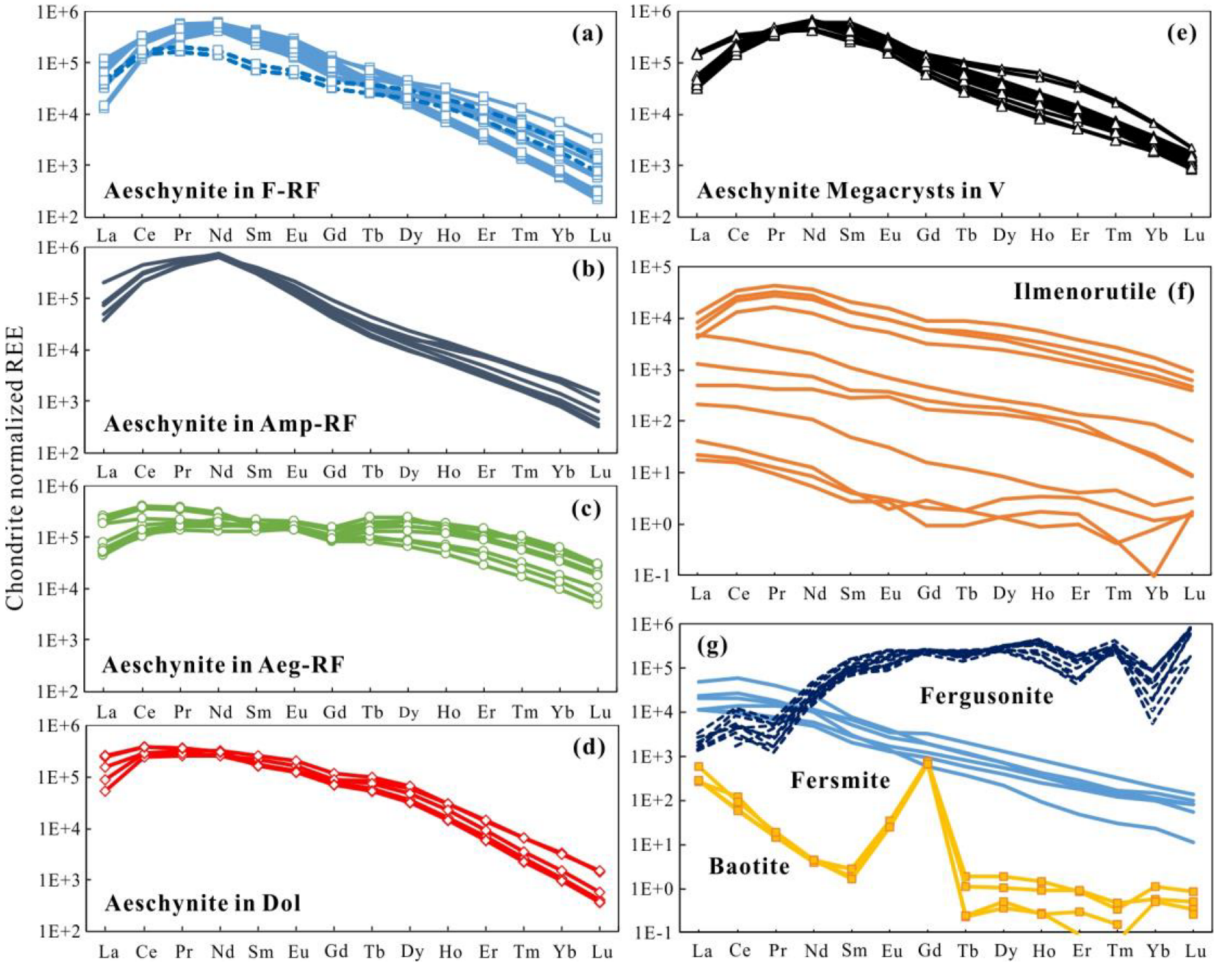

Fig. 9. Chondrite normalized REE patterns of Bayan Obo Nb-bearing minerals (analyzed by LA-ICPMS) a) Aeschynite in the fluorite-rich REE-Fe ores (F-RF); b) aeschynite in the sodium-amphibole-rich REE-Fe ores (Amp-RF); c) aeschynite in the aegirine-rich REE-Fe ores (Aeg-RF); d) aeschynite in the slightly-altered ore-hosting dolomite (Dol); e) aeschynite megacrysts in the vein-type of ores (V); f) variable REE patterns of ilmenorutile from the aegirine-rich Nb-REE ores (lower ΣREE) and fluorite-rich REE-Nb ores (higher ΣREE); g) chondrite normalized REE patterns of fersmite, baotite (based on LA-ICPMS) and fergusonite (based on EMPA).

experimental determination. But during our digestion of aeschynite, it dissolved prominently in the mixture of HF and oxidizing acid solution (e.g. inverse aqua regia), rather than solution of any single acid. Increasing HF concentration or decreasing pH has also been experimentally demonstrated beneficial to the digestion of Nb_2O_5 (Timofeev et al., 2015). Based on thermodynamic experiment, REE would be mainly transported by F^-, Cl^-, CO_3^{2-} and SO_4^{2-} in aqueous solutions, among which F- is significant for Nb transport, while the rest are noneffective for dissolution of Nb oxides in our pretreatment and available papers (Smith and Spratt 2012; Migdisov et al., 2016). Therefore, REE-rich but F-poor fluids, e.g. carbonatite-derived CO_2-rich carbothermal fluids, are unable to carry substantial Nb. While HF-rich oxidizing aqueous hydrothermal fluids are proper candidates for Nb transport. The distinct complexing preference of REE and Nb in aqueous solution may cause their differentiated mineralization that has been occasionally observed in Bayan Obo.

6.4. Age of Paleozoic hydrothermal Nb mineralization

Based on petrographic and geochemical evidence, the Mesoproterozoic and Paleozoic Nb mineralization have been classified. Due to the small grain size and scarcity of aeschynite and columbite in the aegirine-rich ores and slightly-altered ore-hosting dolomite, the age of Mesoproterozoic Nb-mineralization was not directly determined. Isochron ages of the Paleozoic aeschynite megacrysts have been calculated in this study. These ages are displayed in Table 9 and Fig. 13a and b. Four of the seven aeschynite megacrysts are able to constrain a Rb-Sr isochron age of 290.3 ± 15.1 Ma (MSWD = 8.2). Meanwhile, five of the seven samples provide a Sm-Nd isochron age of 658.4 ± 36.0 Ma (MSWD = 3.8).

6.4.1. Rb-Sr isochron age of aeschynite megacrysts

The interpretation of these isochron ages would be oversimplified, if regarding them as the forming age of Paleozoic aeschynite. The Rb-Sr isochron age of aeschynite megacrysts is similar to but slightly older than the age of Permian granite-diorite (263–281 Ma) at Bayan Obo, which was caused by collision between the Siberian Plate and the North China Craton (Fan et al., 2009). Meanwhile, a series of Permian granite-diorite stocks emplaced the north margin of North China Craton during the closure of Paleo-Asian Ocean: Jibei diorite with zircon U-Pb age of 288(± 5)-280(± 6) Ma (Wang et al., 2007); Guyang granite with zircon U-Pb age of 282 ± 3 Ma (Zeng et al., 2008). The Rb-Sr isochron age of aeschynite megacrysts is slightly older than the above stocks, may because of the limited aeschynite samples and relatively poor precision of Rb-Sr dating compared with *in situ* zircon dating. But it is more likely that the Rb-Sr age of aeschynite was modified by the intrusion of Permian granite.

However, it still lacks of evidence about the accurate forming age of these aeschynite. Contradict evidences are common in Bayan Obo ores. For example, the aeschynite megacrysts in this study were mostly

Table 8
REE, other minor and trace element composition (ppm) of aeschynite monominerals analyzed by ICP-MS.

	19BY01	19BY02	19BY03	19BY04	19BY05	19BY06	19BY07	BCR-2
Sc	2.0	8.6	10.0	2.8	4.9	2.2	99.6	32.2
Ti	268,463	44,735	81,132	22,187	124,721	103,368	32,328	14,575
Rb	0.2	23.9	21.3	15.7	19.4	18.1	54.9	46.1
Sr	242.4	719.8	877.1	4439	249.9	3077	2869	327.3
Y*	136.0	9345	8727	7881	7388	8141	9728	33.2
Zr	1.4	35.6	33.0	45.1	24.9	48.5	31.8	239.6
Nb	3068	527.1	1816	182.3	6649	3467	36,294	3.9
Mo	1.5	0.2	0.2	u.d.	0.3	0.2	0.1	369.2
Sn	131.3	226.5	436.4	38.9	916.4	145.4	59.3	2.7
Sb	u.d.	u.d.	u.d.	u.d.	0.7	0.2	u.d.	0.5
Te	u.d.	2.2	2.6	0.7	2.3	0.2	0.7	1.3
Cs	u.d.	0.1	u.d.	u.d.	u.d.	u.d.	u.d.	1.3
Ba	1221	811.7	1498	18,744	375.1	31,739	4413	796.4
La*	307.3	3347	4106	21,009	2345	20,731	13,572	23.5
Ce*	1757	44,769	54,855	94,214	31,975	111,553	72,306	52.9
Pr*	435.1	15,529	17,355	17,220	11,196	20,082	13,630	6.2
Nd*	2837	126,425	141,006	90,010	91,412	116,450	67,746	27.0
Sm*	501.8	33,448	36,039	17,283	24,589	23,194	14,301	6.0
Eu*	78.3	5975	6149	3875	4424	4823	3651	1.7
Gd*	130.8	9935	9805	8127	7496	9769	7935	6.5
Tb*	12.2	986.5	999	892.5	761.0	1106	1114	1.0
Dy*	49.7	4081	4106	3608	3116	4493	5189	6.2
Ho*	6.5	528.8	536.9	441.9	408.2	524.8	683.1	1.2
Er*	13.3	972.4	1024	750.1	779.6	851.7	1194	3.5
Tm*	1.0	73.0	68.0	53.5	58.7	48.1	86.3	0.5
Yb*	4.1	253.1	251.0	179.5	209.5	153.2	267.6	3.2
Lu*	0.3	17.6	16.9	12.6	15.4	9.7	17.5	0.4
Hf	0.4	6.9	7.8	9.1	7.5	8.3	9.0	7.7
Ta	0.3	0.3	0.5	0.5	0.8	3.6	23.9	1.1
Re	u.d.	0.1	0.1	0.1	0.1	0.1	0.2	u.d.
Pb	12.3	1397	1546	566	1680	784.4	358.6	11.0
Th*	411.1	44,405	49,553	7020	29,287	7070	8908	4.6
U	1.4	146.3	176.5	694.4	203.3	847.3	275.6	2.1

* Elements with asterisk were analyzed after extra about 500-times dilution of the diluted solution prepared for other elements.

collected from aeschynite-calcite veins cutting through other types of ores. However, at Bayan Obo, typical early Paleozoic vein-type of ores (~430–440 Ma) are generally composed of megacrysts of pyrite (other sulfides are not as common), fluorite, Na-amphibole, aegirine, fluorocarbonates (e.g. huanghoite), barite and phlogopite occasionally. Among all above minerals, pyrite, molybdenite and phlogopite have been used for the directly dating of the typical vein-type of ores, and all results support a 430–440 Ma modification event inside the ore-hosting dolomite (Chao et al., 1992; Liu et al., 1996; Liu et al., 2004; Hu et al., 2009). Besides, Chao et al. (1991) has drawn a Th-Pb isochron of huanghoite (2 point) and aeschynite (2 point) with age of 438 ± 25 Ma, supporting a ~440 Ma Nb mineralization event. These huanghoite and aeschynite were collected from an aegirine vein cutting through the banded ores. However, in both Smith et al. (2014) (Fig. 2b in that study) and this study, aeschynite megacrysts were often collected from calcite-rich veins, which have different mineral assemblages from the typical early Paleozoic veins. It is uncommon for aeschynite in the calcite vein to associate with sulfide, phlogopite or huanghoite which have solid forming-age. Therefore, there is still a lack of direct evidence whether the calcite-aeschynite vein was formed simultaneously or co-genetic to the typical pyrite-rich veins between 430 and 440 Ma.

On the other hand, it is quite likely that the 290 Ma Rb-Sr age in this study is a modified age of formerly crystalized aeschynite. The Permian granite has influenced the Bayan Obo ore-hosting dolomite extensively, which is always ignored by researchers that tries to simplify a two-stage metallogenic model. In the deeply drilled ore-hosting dolomite, phlogopite has a Rb-Sr isochron age of about 309 ± 12 Ma (Yang et al., 2007), supporting the extensive modification of Permian granite to the ore-hosting dolomite. However, it is also possible that the Permian age of aeschynite megacrysts indicates a Nb remobilization event within the Nb-bearing ore-hosting dolomite when granite intruded at about

Table 9
Rb-Sr, Sm-Nd isotopic ratios of aeschynite monominerals.

	19BY01	19BY02	19BY03	19BY04	19BY05	19BY06	19BY07
Rb (ppm)	0.20	23.9	21.3	15.7	19.4	18.1	54.9
Sr (ppm)	242	720	877	4439	250	3077	2869
$^{87}Rb/^{86}Sr$	0.002	0.096	0.070	0.010	0.225	0.017	0.055
$^{87}Sr/^{86}Sr$	0.706381	0.706254	0.706231	0.705954	0.706381	0.705956	0.705921
(± $2s_m$)	0.000010	0.000011	0.000011	0.000008	0.000010	0.000009	0.000011
Sm (ppm)	502	33,448	36,039	17,283	24,589	23,194	14,301
Nd (PPm)	2837	126,425	141,006	90,010	91,412	116,450	67,746
$^{147}Sm/^{144}Nd$	0.1069	0.1600	0.1545	0.1161	0.1626	0.1204	0.1276
$^{143}Nd/^{144}Nd$	0.511642	0.512762	0.511804	0.511649	0.511870	0.511656	0.511619
(± $2s_m$)	0.000008	0.000008	0.000009	0.000009	0.000008	0.000009	0.000009

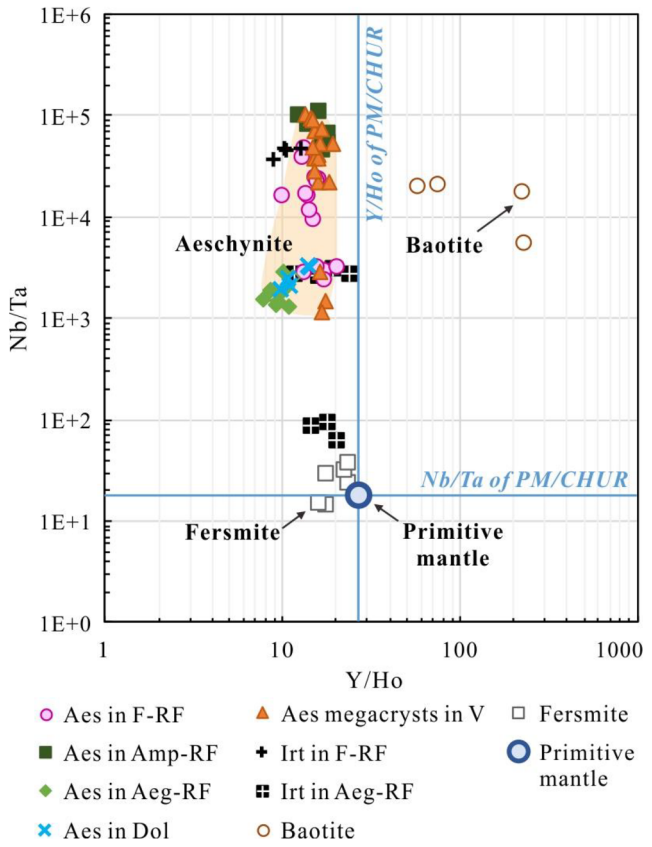

Fig. 1.0. Y/Ho ratios of Bayan Obo Nb-bearing minerals (Abbreviations see the above figures) Shadowed area represents aeschynite.

270 Ma. The aeschynite megacrysts are characterized by less radiogenic $^{87}Sr/^{86}Sr$ ratios (290.3 Ma) compared with granite, but more radiogenic Sr composition than that of local carbonatite, the fresh and the altered ore-hosting dolomite. Therefore, crustal contamination of the Paleozoic Nb-bearing hydrothermal fluids, either from the metasedimentary rocks or the granite stock, have to be involved in the formation of these aeschynite. The granite might provide heat that reset the Rb-Sr system and material that increase the $^{87}Sr/^{86}Sr$ ratios. The distribution of Nb ore is rather random in the open pits, but generally with low Nb grade and high REE grade. Fe-poor tail rocks around the Bayan Obo open pits (East and Main Open Pits) contain rare earth oxides (REO) in the range of 0.83–5.37 wt%, while the average weight percentage of Nb_2O_5 is < 0.117 wt% (0.055–0.117 wt%) (Hao, 2017). Meanwhile, there are several major Nb ore bodies located outside the current open pits and next to the contact zone between the Permian granite stock and the eastern frontier of ore-hosting dolomite. Taking the so-called 2# Nb ore body on the contact zone as an example, the ore-hosting dolomite contains only 0.35 wt% of REO while extremely enriching Nb_2O_5 (0.35 wt%) (Zhang and Mu, 2006). This evidence refers a Nb re-enrichment process within the ore-hosting dolomite under influence of Permian granite intrusion, without prominent REE re-enrichment. Despite of this, the Paleozoic Nb resources was unlikely to be originated from the Permian granite, which is not even alkaline as some Nb-Ta-rich granites in Southern China, but rather originated from remobilization of precursory Nb resources within the ore-hosting dolomite, under influence of heats or hydrothermal fluids subjected to the Permian granitic melt. Afterall, the average Nb composition of bulk Bayan Obo granite is only 16–19 ppm, an order of magnitude lower than local carbonatite dykes, excluding this genetic possibility (Zhang et al., 2003).

In summary, the classic two-stage metallogenic model is primarily designed for REE mineralization. The mineralization or remobilization of Nb and Fe may not be restricted by this model, and has never been seriously discussed. As the first introduction of REE and Nb to the ore-hosting dolomite, the Mesoproterozoic REE-Nb mineralization related to carbonatite magmatism is well accepted. The early Paleozoic (~430 Ma) REE mineralization, represented by typical REE-pyrite-rich veins, has been demonstrated with solid geochronological evidence. The 440–430 Ma Nb mineralization in the aegirine vein was reported by Chao et al. (1991). There are two possible geological processes that would cause the local Paleozoic Nb mineralization/remobilization in the calcite veins: the ~430 Ma subduction or the ~270 Ma granite intrusion. Neither interpretation was able to be excluded with overwhelming evidence yet. It is worthy to stress again that the Paleozoic Nb mineralization was remobilization of carbonatite-introduced Nb within the ore-hosting dolomite. There were no external Nb resources originated from the Permian granite magma.

6.4.2. Sm-Nd isochron age of aeschynite megacrysts

There is no reported geological event corresponding to the Sm-Nd isochron age of this study, which is intermediate between the age of Mesoproterozoic carbonatite intrusion (~1.3 Ga) and the incipient closure of the Paleo-Asian Ocean (~430 Ma). Therefore, the age of 658.4 Ma should be regarded as an apparent age as result of incomplete reset of the Sm-Nd isotopic system.

Based on the $^{143}Nd/^{144}Nd$ evolution line of these aeschynite (Fig. 13c), the lines of five samples intersect each other at around 658 Ma, and the intersection lies on the Nd evolution line of Bayan Obo REE repository (BYRR). The BYRR as a whole, due to the significant REE background in different kinds of ores and ore-hosting rocks, generally has persistent Sm-Nd isotopic evolution towards later modification (Zhu et al., 2015). However, specific monominerals in BYRR, such as fluorite, fluorocarbonate, monazite, phlogopite or aeschynite in this study, might reach local re-equilibrium of Sm-Nd isotopes after heat events and prominent REE re-mobilization. At Bayan Obo, only the Paleozoic subduction event has reset the Sm-Nd systems of above minerals extensively (Chao et al., 1991; Hu et al., 2009; Liu et al., 2018b), indicating there is no prominent REE-remobilization event during the granite activity. Since the intersection of aeschynite lines was situated on the Nd evolution line of BYRR, REEs in the aeschynite were originated from the REE repository that was introduced to by Mesoproterozoic carbonatite melts. Most aeschynite megacrysts inherit REE from both the Mesoproterozoic and the Paleozoic REE mineralization, with an intermediate Sm-Nd isochron age between two major REE mineralization events. As exception, 19BY07 has a Nd evolution line crossing the BYRR line at ~430 Ma, indicating that Paleozoic REE mineralization provided majority of its REE.

6.4.3. Future research on Paleozoic Nb mineralization

Since neither Rb-Sr or Sm-Nd isochron age in this study was able to provide precise forming age of aeschynite megacrysts, it is important to distinguish the contribution of early Paleozoic hydrothermal event (~430 Ma) from that of the granite intrusion (~270 Ma) in the future research. The Nb-rich ore-hosting dolomite near the eastern contact zone has potential to verify the granite-related Nb remobilization process. This process is special because the Nb enrichment is independent from the REE enrichment. The fractionation between REE and Nb is critical to further discussion on the carbonatite-related REE-Nb mineralization relationship.

7. Conclusions

1. Multiple kinds of Nb-bearing minerals in the ore and ore-hosting dolomite of the Bayan Obo REE-Nb-Fe deposits, including aeschynite, ilmenorutile, baotite and fergusonite, have hydrothermal origins, while fersmite presents igneous origin and columbite may record both the magmatic and hydrothermal origins which needs further research.

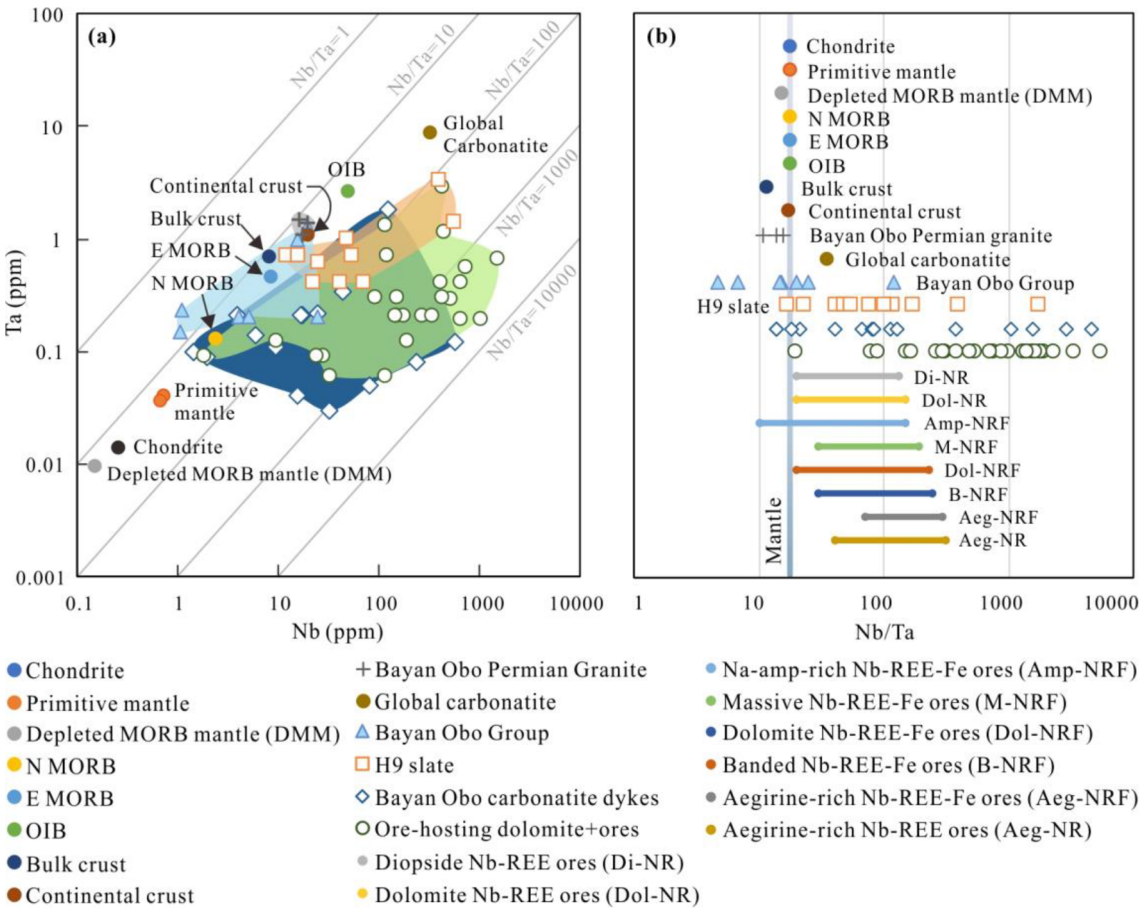

Fig. 11. Nb and Ta composition of Nb-bearing minerals, ores, ore-hosting dolomite and other geological repositories. a) Nb and Ta composition of Nb-bearing minerals, Chondrite, primitive mantle, N MORB and E MORB, depleted MORB mantle (DDM), OIB, crust, global and local carbonatite, local granite, Bayan Obo Group, ores and ore-hosting dolomite (Sun and McDonough, 1989; McDonough and Sun, 1995; Wedepohl, 1995; Rudnick and Gao, 2003; Zhang et al., 2003; Workman and Hart, 2005; Yang et al., 2011a; Sun et al., 2014); b) Nb/Ta ratios of the above geological repositories.

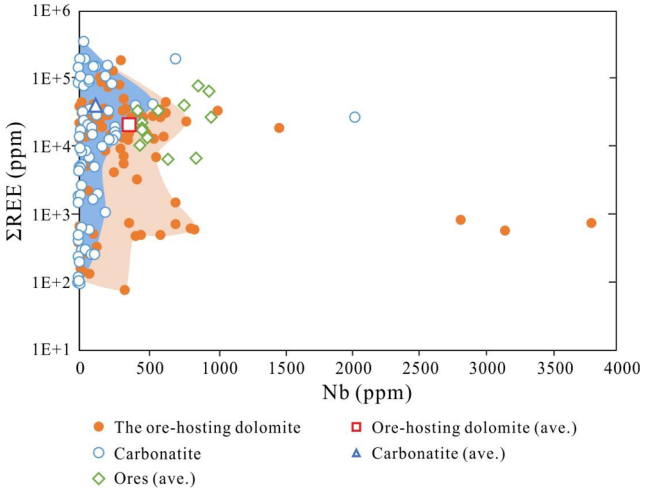

Fig. 12. ΣREE and Nb fractionation in the ore-hosting dolomite, carbonatite dykes and ores. Trace element data has been published in Le Bas et al. (1992, 1997), Wang et al. (2002), Yang et al. (2003, 2009, 2011a), Lai et al. (2012), Lai and Yang (2013), Ling et al. (2013) and Sun et al. (2014). Average ΣREE and Nb composition of the above rocks were calculated.

2. Aeschynite was classified into three groups according to major and REE composition. Aeschynite of Group 1 was formed from Paleozoic hydrothermal fluids. Those of Group 2 and 3 precipitated from Mesoproterozoic carbonatite-derived hydrothermal fluids.
3. Aqueous hydrothermal processes, both the Mesoproterozoic and the Paleozoic, are far more significant for the Bayan Obo Nb enrichment compared with Mesoproterozoic carbonatite magmatism. Meanwhile, REE was able to precipitate extensively during both the carbonatite-related magmatic and hydrothermal processes. The Nb-Ta fractionation in ores was inherited from Mesoproterozoic carbonatite melt as a primary geochemical characteristic.
4. The differentiated REE-Nb mineralization was developed during hydrothermal processes. Nb mineralization was generally postdating the LREE mineralization at the same stage. The formation of aeschynite (Group 1), ilmenorutile and fergusonite was later than Paleozoic REE mineralization. Mesoproterozoic REE mineralization occurred ahead of the aeschynite (Group 3) and baotite, while simultaneous to aeschynite of Group 2 as exception.
5. The aeschynite megacrysts in the calcite veins have a modified Rb-Sr isochron age (290.3 ± 15.1 Ma) under the influence of Permian granite intrusion. Paleozoic Nb mineralization might occur during the ~440 Ma remobilization forming the vein-type of ores, or alternatively the ~270 Ma remobilization during the granite intrusion. No external Nb was introduced from the granite melt. REE in the aeschynite megacrysts was originated from formerly multistage REE mineralization, presenting an intermediate apparent Sm-Nd isochron age (658.4 ± 36.0 Ma) between the Mesoproterozoic and the Paleozoic REE mineralization events.

CRediT authorship contribution statement

Shang Liu: Conceptualization, Methodology, Writing - original

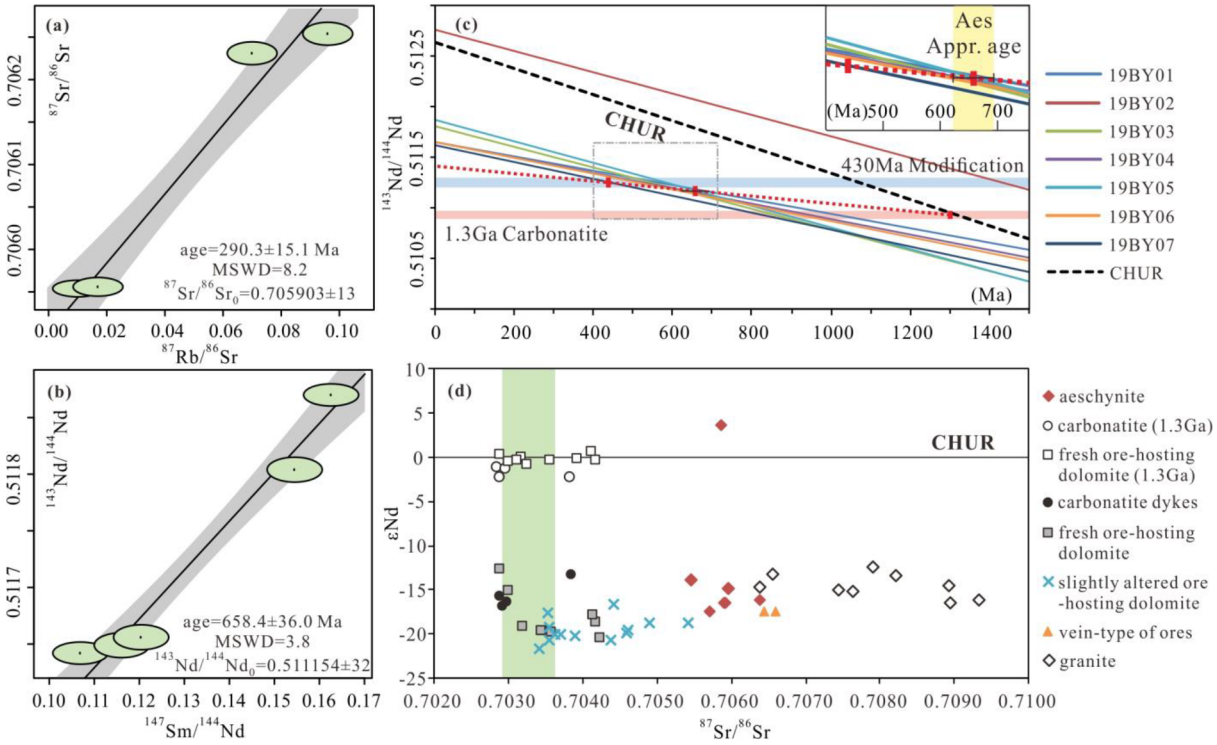

Fig. 13. Rb-Sr and Sm-Nd isotopic composition of aeschynite megacrysts a) Rb-Sr isochron age of aeschynite; b) Sm-Nd isochron age of aeschynite; c) Nd isotopic evolution lines of aeschynite megacrysts and the Bayan Obo REE repository, and the Nd evolution line of the Bayan Obo REE repository was cited from Zhu et al. (2015); d) initial Sr-Nd isotopic ratios of aeschynite megacrysts (this study), local Mesoproterozoic carbonatite dykes and ore-hosting dolomite, Paleozoic vein-type of ores and Permian granite (Zhang et al., 2003; Le Bas et al., 2007; Yang et al., 2011b).

draft. **Lin Ding:** Writing - review & editing, Supervision. **Hong-Rui Fan:** Writing - review & editing, Conceptualization. **Kui-Feng Yang:** Conceptualization, Investigation. **Yan-Wen Tang:** Methodology, Resources. **Hai-Dong She:** Investigation, Resources. **Mei-zhen Hao:** Resources.

Declaration of Competing Interest

The authors declare that they have no known competing financial interests or personal relationships that could have appeared to influence the work reported in this paper.

Acknowledgements

We are grateful to Prof. Zhan-Feng Yang, Mr. Qi-Wei Wang, Mr. Yong-Gang Zhao and M.S. Hong-Tao Li for their kindly assistance during the field trip. Without careful and appreciated help from the following people, the pretreatment of samples cannot be accomplished: Ms. Ping Xiao, Mr. Chang-Fu Yu, Ms. Cong-Hui Xiong, Dr. Wan-Feng Chen, Ms. Shu-Fen Yang. We also received a lot of professional guidance from Prof. Fu-Kun Chen, Dr. Ting-Guang Lan, Dr. Bing Wu, Ms. Zhi-Hui Dai, Ms. Xiao-Li Yan, Mr. Yun-Long Pang, Dr. Kai-Xuan Li and Mr. Jun-Jie Han during the analytical experiment. This research was financially supported by the National Natural Science Foundation of China (41902066; 41930430) and the Fundamental Research Funds for the Central Universities of China (Lzujbky-2019-pd06; 2022019zr106).

Appendix A. Supplementary data

Supplementary data to this article can be found online at https://doi.org/10.1016/j.precamres.2020.105864.

References

Bai, G., Yuan, Z.X., Wu, C.Y., Zhang, Z.Q., Zheng, L.X., 1996. Demonstration on the geological features and genesis of the Bayan Obo ore deposit. Geology Publishing House, Beijing, p. 104. (In Chinese with English abstract).

Bau, M., 1996. Controls on the fractionation of isovalent trace elements in magmatic and aqueous systems: evidence from Y/Ho, Zr/Hf, and lanthanide tetrad effect. Contrib. Mineral. Petrol. 123, 323–333.

Bermanec, V., Tomašić, N., Kniewald, G., Back, M.E., Zagler, G., 2008. Nioboaeschynite-(Y), a new member of the aeschynite group from the Bear Lake Diggings, Haliburton County, Ontario, Canada. Can. Mineral. 46, 395–402.

Černý, P., Ercit, T.S., 1989. Mineralogy of Niobium and Tantalum: crystal chemical relationships, paragenetic aspects and their economic implications. In: Möller, P., Černý, P., Saupé (Eds.), Lanthanides, Tantalum and Niobium. Springer-Verlag, Berlin, pp. 27–79.

Bühn, B., Rankin, A.H., 1999. Composition of natural, volatile-rich Na-Ca-REE-Sr carbonatitic fluids trapped in fluid inclusion. Geochimica et Cosmochimica Acta 63, 3781–3797.

Chakhmouradian, A.R., 2006. High-field-strength elements in carbonatitic rocks: Geochemistry, crystal chemistry and significance for constraining the sources of carbonatites. Chem. Geol. 235, 138–160.

Chao, E.C.T., Tatsumoto, M., Martin, J.A., Back, J.M., McKee, E.H., Ren, Y.C., 1991. Multiple lines of evidence for establishing the mineral paragenetic sequence of the Bayan Obo rare earth ore deposit of Inner Mongolia, China. Contrib. Geol. Mineral Resour. Res. 6, 1–17 (In Chinese with English abstract).

Chao, E.C.T., Back, J.M., Minkin, J.A., 1992. Host-rock controlled epigenetic, hydrothermal metasomatic origin of the Bayan Obo REE-Fe-Nb ore deposit, Inner Mongolia, P.R.C. Appl. Geochem. 7, 443–458.

Chen, F., Hegner, E., Todt, W., 2000. Zircon ages and Nd isotopic and chemical compositions of orthogneisses from the Black Forest, Germany: evidence for a Cambrian magmatic arc. Int. J. Earth Sci. 88, 791–802.

Chen, F., Li, X.H., Wang, X.L., Li, Q.L., Siebel, W., 2007. Zircon age and Nd–Hf isotopic composition of the Yunnan Tethyan belt, southwestern China. Int. J. Earth Sci. 96, 1179–1194.

Chen, W., Liu, H.Y., Lu, J., Jiang, S.Y., Simonetti, A., Xu, C., Zhang, W., 2019. The formation of the ore-hosting dolomite marble from the giant Bayan Obo REE-Nb-Fe deposit, Inner Mongolia: insights from micron-scale geochemical data. Miner. Deposita 4, 1–16.

Cooper, A.F., 1996. Nb-rich baotite in carbonatites and fenites at Haast River, New Zealand. Mineral. Mag. 60, 473–482.

Cordeiro, P.F.O., Brod, J.A., Palmieri, M., Oliveira, C.G., Barbosa, E.S.R., Santos, R.V., Gaspar, J.C., Assis, L.C., 2011. The Catalão I niobium deposit, central Brazil: Resources, geology and pyrochlore chemistry. Ore Geol. Rev. 41, 112–121.

Fan, H.R., Hu, F.F., Yang, K.F., Wang, K.Y., Liu, Y.S., 2009. Geochronology framework of late Paleozoic dioritic-granitic plutons in the Bayan Obo area, Inner Mongolia, and tectonic significance. Acta Petrol. Sin. 25, 2933–2938.
Fan, H.R., Hu, F.F., Yang, K.F., Pirajno, F., Liu, X., Wang, K.Y., 2014. Integrated U-Pb and Sm–Nd geochronology for a REE-rich carbonatite dyke at the giant Bayan Obo REE deposit, Northern China. Ore Geol. Rev. 63, 510–519.
Fan, H.R., Yang, K.F., Hu, F.F., Liu, S., Wang, K.Y., 2016. The giant Bayan Obo REE-Nb-Fe deposit, China: controversy and ore genesis. Geosci. Front. 7, 335–344.
Fei, H.C., 2005. Genesis study of the alkali rock series, Rare Earth Element and Magnetite deposit in Bayan Obo, Inner Mongolia. (Doctoral dissertation). China University of Geosciences, Beijing, In Chinese with English abstract).
Giovannini, A.L., Neto, A.C.B., Porto, C.G., Pereira, V.P., Takehara, L., Barbanson, L., Bastos, P.H., 2017. Mineralogy and geochemistry of laterites from the Morro dos Seis Lagos Nb (Ti, REE) deposit (Amazonas, Brazil). Ore Geol. Rev. 88, 461–480.
Hao, M.Z., 2017. Conservation status of rare earth and niobium resources in Baiyunebo Iron Mine waste dump. Sci. Technol. Baotou Steel Corp. 43S, 41–44 (In Chinese with English abstract).
He, H.Y., He, M., Li, J.W., 2018. Analysis of the niobium resources supply and demand pattern in China. China Min. Mag. 27, 1–5 (In Chinese with English abstract).
Hou, X.Z., Yang, Z.F., Wang, Z.J., Wang, W.C., 2018. Study on minerals composition characteristics of Niobium concentrate and distribution of Niobium in Bayan Obo. Nonferrous Metals (Min. Process. Sect.) 2, 4–11 (In Chinese with English abstract).
Hu, F.F., Fan, H.R., Liu, S., Yang, K.F., Chen, F.K., 2009. Samarium-Neodymium and Rubidium-Strontium isotopic dating of veined REE mineralization for the Bayan Obo REE-Nb-Fe deposit, Northern China. Resour. Geol. 59, 407–414.
Hu, L., Li, Y.K., Wu, Z.J., Bai, Y., Wang, A.J., 2019. Two metasomatic events recorded in apatite from the ore-hosting dolomite marble and implications for genesis of the giant Bayan Obo REE deposit, Inner Mongolia, Northern China. J. Asian Earth Sci. 172, 56–65.
Huang, X.W., Zhou, M.F., Qiu, Y.Z., Qi, L., 2015. In-situ LA-ICP-MS trace elemental analyses of magnetite: The Bayan Obo Fe-REE-Nb deposit, North China. Ore Geol. Rev. 65, 884–899.
IGCAS (Institute of Geochemistry, Chinese Academy of Sciences), 1988. The Geochemistry of Bayan Obo Deposit. Science Press, Beijing, pp.164–174. (In Chinese).
Kullerud, K., Zozulya, D., Ravna, E.J.K., 2012. Formation of baotite – a Cl-rich silicate – together with fluorapatite and F-rich hydrous silicates in the Kvaløya lamproite dyke, North Norway. Mineral. Petrol. 105, 145–156.
Lai, X.D., Yang, X.Y., Sun, W.D., 2012. Geochemical constraints on genesis of dolomite marble in the Bayan Obo REE–Nb–Fe deposit, Inner Mongolia: Implications for REE mineralization. J. Asian Earth Sci. 57, 90–102.
Lai, X.D., Yang, X.Y., 2013. Geochemical characteristics of the Bayan Obo giant REE-Nb-Fe deposit: Constraints on its genesis. J. S. Am. Earth Sci. 41, 99–112.
Le Bas, M.J., Keller, J., Tao, K.J., Wall, F., Williams, C.T., Zhang, P.S., 1992. Carbonatite dykes at Bayan Obo, Inner Mongolia, China. Mineral. Petrol. 46, 195–228.
Le Bas, M.J., Spiro, B., Yang, X.M., 1997. Oxygen, carbon and strontium isotope study of the carbonatitic dolomite host of the Bayan Obo Fe-Nb-REE deposit, Inner Mongolia, N China. Mineral. Mag. 61, 531–541.
Le Bas, M.J., Yang, X.M., Taylor, R.N., Spiro, B., Milton, J.A., Zhang, P.S., 2007. New evidence from a calcite-dolomite carbonatite dyke for the magmatic origin of the massive Bayan Obo ore-bearing dolomite marble, Inner Mongolia, China. Mineral. Petrol. 90, 223–248.
Lee, W.J., Wyllie, P.J., 1998. Petrogenesis of carbonatite magmas from mantle to crust, constrained by the system CaO-(MgO + FeO)-($Na_2O + K_2O$)-($SiO_2 + Al_2O_3 + TiO_2$)-CO_2. J. Petrol. 39, 495–517.
Liu, L.S., Gao, L., Du, A.D., Sun, Y.L., 1996. The Re-Os isotopic age of molybdenite from Bayan Obo REE ore deposit. Min. Deposits 15 (2), 188–191 (In Chinese with English abstract).
Ling, M.X., Liu, Y.L., Williams, I.S., Teng, F.Z., Yang, X.Y., Ding, X., Wei, G.J., Xie, L.H., Deng, W.F., Sun, W.D., 2013. Formation of the world's largest REE deposit through protracted fluxing of carbonatite by subduction-derived fluids. Sci. Rep. 3, 1776.
Liu, J., Li, Y., Ling, M.X., Sun, W.D., 2011. Chronology and geological significance of the basement rock of the giant Bayan Obo REE-Nb-Fe ore deposit. Geochimica 40, 209–222 (In Chinese with English abstract).
Liu, S., Fan, H.R., Yang, K.F., Hu, F.F., Rusk, B., Liu, X., Li, X.C., Yang, Z.F., Wang, Q.W., Wang, K.Y., 2018a. Fenitization in the giant Bayan Obo REE-Nb-Fe deposit: Implication for REE mineralization. Ore Geol. Rev. 94, 290–309.
Liu, S., Fan, H.R., Yang, K.F., Wang, K.Y., Hu, F.F., Wang, K.Y., Chen, F.K., Yang, Y.H., Yang, Z.F., Wang, Q.W., 2018b. Mesoproterozoic and Paleozoic hydrothermal metasomatism in the Bayan Obo REE-Nb-Fe deposit: constrains from trace elements and Sr-Nd isotope of fluorite and preliminary thermodynamic calculation. Precambr. Res. 311, 228–246.
Liu, S., Fan, H.R., Groves, D.I., Yang, K.F., Yang, Z.F., Wang, Q.W., 2020. Multiphase carbonatite-related magmatic and metasomatic processes in the genesis of the ore-hosting dolomite in the giant Bayan Obo REE-Nb-Fe deposit. Lithos 354–355, 105359.
Liu, T.G., 1985. Geological and geochemical character of Baiyun Ebo rauhaugite. Acta Petrol. Sin. 1, 15–28 (In Chinese with English abstract).
Liu, Y., Yang, G., Chen, J., Du, A., Xie, Z., 2004. Re-Os dating of pyrite from giant Bayan Obo REE-Nb-Fe deposit. Chin. Sci. Bull. 49, 2627–2631.
Liu, Y.F., Bagas, L., Nie, F.J., Jiang, S.H., Li, C., 2016. Re–Os system of black schist from the Mesoproterozoic Bayan Obo Group, Central Inner Mongolia, China and its geological implications. Lithos 261, 296–306.
Liu, Y.S., Hu, Z.C., Gao, S., Günther, D., Xu, J., Gao, C.G., Chen, H.H., 2008. In situ analysis of major and trace elements of anhydrous minerals by LA-ICP-MS without applying an internal standard. Chem. Geol. 257, 34–43.
Mackay, D.A.R., Simandl, G.J., 2014. Geology, market and supply chain of niobium and tantalum-a review. Miner. Deposita 49, 1025–1047.
McDonough, W.F., Sun, S.S., 1995. The composition of the earth. Chem. Geol. 120, 223–253.
Migdisov, A., Williams-Jones, A.E., Brugger, J., Caporuscio, F.A., 2016. Hydrothermal transport, deposition, and fractionation of the REE: experimental data and thermodynamic calculations. Chem. Geol. 439, 13–42.
Nasraoui, M., Bilal, E., 2000. Pyrochlores from the Lueshe carbonatite complex (Democratic Republic of Congo): a geochemical record of different alteration stages. J. Asian Earth Sci. 18, 237–251.
Neumann, R., Medeiros, E.B., 2015. Comprehensive mineralogical and technological characterisation of the Araxá (SE Brazil) complex REE (Nb-P) ore, and the fate of its processing. Int. J. Miner. Process. 144, 1–10.
Ren, Y., Yang, X., Wang, S., Öztürk, H., 2019. Mineralogical and geochemical study of apatite and dolomite from the Bayan Obo giant Fe-REE-Nb deposit in Inner Mongolia: New evidences for genesis. Ore Geol. Rev. 109, 381–406.
Rudnick, R.L., Gao, S., 2003. Composition of the continental crust. In: Holland, H.D., Turekian, K.K. (Eds.), Treatise on Geochemistry. Elsevier Science, pp. 1–64.
Silvola, J., 1970. Ilmenorutile and strüverite from Penikoja, Somero, SW Finland. Bull. Geol. Soc. Finland 42, 33–36.
Simandl, G.J., Burt, R.O., Trueman, D.L., Paradis, S., 2018. Economic geology models 2. Tantalum and niobium: deposits, resources, exploration methods and market – a primer for geoscientists. Geosci. Can. 45, 85–96.
Smith, M.P., Henderson, P., Campbell, L.S., 2000. Fractionation of the REE during hydrothermal processes: Constraints from the Bayan Obo Fe-REE-Nb deposit, Inner Mongolia, China. Geochim. Cosmochim. Acta 64, 3141–3160.
Smith, M., Spratt, J., 2012. The chemistry of Niobium mineralization at Bayan Obo, Inner Mongolia, China: Constraints on the hydrothermal precipitation and alteration of Nb-minerals. Acta Geol. Sin. 86, 700–722.
Smith, M., Campbell, L.S., Kynicky, J., 2014. A review of the genesis of the world class Bayan Obo Fe–REE–Nb deposits, Inner Mongolia, China: Multistage processes and outstanding questions. Ore Geol. Rev. 64, 459–476.
Sun, S.S., McDonough, W.F., 1989. Chemical and isotopic systematics of oceanic basalts: implications for mantle composition and processes. Geol. Soc. Lond. Spec. Publ. 42, 313–345.
Sun, J., Zhu, X.K., Chen, Y.L., Fang, N., Li, S.Z., 2014. Is the Bayan Obo ore deposit a micrite mound? A comparison with the Sailinhudong micrite mound. Int. Geol. Rev. 56, 1720–1731.
Tao, K.J., Yang, Z.M., Zhang, P.S., Wang, W.Z., 1998. Systematic geological investigation on carbonatite dykes in Bayan Obo, Inner Mongolia, China. Sci. Geol. Sin. 33, 73–83 (In Chinese with English abstract).
Timofeev, A., Migdisov, A.A., Williams-Jones, A.E., 2015. An experimental study of the solubility and speciation of niobium in fluoride-bearing aqueous solutions at elevated temperature. Geochim. Cosmochim. Acta 158, 103–111.
Timofeev, A., Williams-Jones, A.E., 2015. The Origin of Niobium and Tantalum Mineralization in the Nechalacho REE Deposit, NWT, Canada. Econ. Geol. 110, 1719–1735.
Tindle, A.G., Breaks, F.W., 2000. Columbite-tantalite mineral chemistry from rare-element granitic pegmatites: Separation Lake area, N.W. Ontario, Canada. Mineral. Petrol. 70, 165–198.
U.S. Geological Survey, 2019. Mineral commodity summaries 2019, U.S. Geological Survey, Reston, pp. 114-115.
Wallace, M.E., Green, D.H., 1998. An experimental determination of primary carbonatite magma composition. Nature v. 335, 343–346.
Walter, B.F., Parsapoor, A., Braunger, S., Marks, M.A.W., Wenzel, T., Martin, M., Markl, G., 2018. Pyrochlore as a monitor for magmatic and hydrothermal processes in carbonatites from the Kaiserstuhl volcanic complex (SW Germany). Chem. Geol. 498, 1–16.
Wang, H.C., Zhao, F.Q., Li, H.M., Sun, L.X., Miao, L.C., Ji, S.P., 2007. Zircon SHRIMP U-Pb age of the dioritic rocks from northern Hebei: the geological records of late Paleozoic magmatic arc. Acta Petrol. Sin. 23, 597–604 (In Chinese with English abstract).
Wang, K.Y., Fan, H.R., Xie, Y.H., 2002. Geochemistry of REE and other trace elements of the carbonatite dykes at Bayan Obo: implication for its formation. Acta Petrol. Sin. 18, 340–348 (In Chinese with English abstract).
Wang, K., Fang, A., Zhang, J., Yu, L., Dong, C., Zan, J., Hao, M., Hu, F., 2019. Genetic relationship between fenitized ores and hosting dolomite carbonatite of the Bayan Obo REE deposit, Inner Mongolia, China. J. Asian Earth Sci. 174, 189–204.
Wedepohl, K.H., 1995. The composition of the continental crust. Geochim. Cosmochim. Acta 59, 1217–1232.
Workman, R.K., Hart, S.R., 2005. Major and trace element composition of the depleted MORB mantle (DMM). Earth Planet. Sci. Lett. 231, 53–72.
Wu, M.Q., Samson, I.M., Zhang, D.H., 2018. Textural features and chemical evolution in ta-nb oxides: implications for deuteric rare-metal mineralization in the yichun granite-marginal pegmatite, Southeastern China. Econ. Geol. 113, 937–960.
Xiao, R., Fei, H., Wang, A., Yang, F., Yan, K., 2012. Formation and geochemistry of the ore-bearing alkaline volcanic rocks in the Bayan Obo REE-Nb-Fe deposit, Inner Mongolia, China. Acta Geol. Sin. 86, 735–752 (In Chinese with English abstract).
Xie, L., Wang, Z., Wang, R., Zhu, J., Che, X., Gao, J., Zhao, X., 2018. Mineralogical constraints on the genesis of W-Nb–Ta mineralization in the Laiziling granite (Xianghualing district, south China). Ore Geol. Rev. 95, 695–712.
Yang, K.F., Fan, H.R., Hu, F.F., Li, X.H., Liu, J.Y., Zhao, Y.G., Liu, S., Wang, K.Y., 2007. Skarnization age in the giant Bayan Obo REE-Nb-Fe ore district, Inner Mongolia, China: Rb-Sr isochron dating on single-grain phlogopite. Acta Petrol. Sin. 23, 1018–1022.
Yang, K.F., Fan, H.R., Santosh, M., Hu, F.F., Wang, K.Y., 2011a. Mesoproterozoic

carbonatitic magmatism in the Bayan Obo deposit, Inner Mongolia, North China: Constraints for the mechanism of super accumulation of rare earth elements. Ore Geol. Rev. 40, 122–131.
Yang, K.F., Fan, H.R., Santosh, M., Hu, F.F., Wang, K.Y., 2011b. Mesoproterozoic mafic and carbonatitic dykes from the northern margin of the North China Craton: Implications for the final breakup of Columbia supercontinent. Tectonophysics 498, 1–10.
Yang, K., Fan, H., Pirajno, F., Li, X., 2019. The Bayan Obo (China) giant REE accumulation conundrum elucidated by intense magmatic differentiation of carbonatite. Geology 47, 1198–1202.
Yang, X.M., Yang, X.Y., Zheng, Y.F., Le Bas, M.J., 2003. A rare earth element-rich carbonatite dyke at Bayan Obo, Inner Mongolia, North China. Mineral. Petrol. 78, 93–110.
Yang, X.Y., Sun, W.D., Zhang, Y.X., Zheng, Y.F., 2009. Geochemical constraints on the genesis of the Bayan Obo Fe–Nb–REE deposit in Inner Mongolia, China. Geochim. Cosmochim. Acta 73, 1417–1435.
Yang, X., Lai, X., Pirajno, F., Liu, Y., Ling, M., Sun, W., 2017. Genesis of the Bayan Obo Fe-REE-Nb formation in Inner Mongolia, North China Craton: a perspective review. Precambr. Res. 288, 39–71.
Yang, Z.M., Smith, M., Henderson, P., Le Bas, M.J., Tao, K.J., Zhang, P.S., 2001. Compositional variation of aeschynite-group minerals in the Bayan Obo Nb-REE-Fe ore deposit, Inner Mongolia, China. Eur. J. Mineral. 13, 1207–1214.
Zeng, J.J., Zheng, Y.Y., Qi, J.H., Dai, F.H., Zhang, G.Y., Pang, Y.C., Wu, B., 2008. Foundation and geological significance of Adakitic granite at Guyang of Inner Mongolia. J. China Univ. Geosci.-Earth Sci. 33, 755–763 (In Chinese with English abstract).
Zhang, P.S., Tao, K.J., 1987. Characteristics of the Fergusonite Group and Aeschynite Group minerals in China. J. Chin. Rare Earth Soc. 5, 1–7 (In Chinese with English abstract).
Zhang, P.S., Tao, K.J., Yang, Z.M., 2000. Nb-Ta mineralogical investigations in China. Geol. J. China Univ. 6, 126–131 (In Chinese with English abstract).
Zhang, Q.F., Mu, X.D., 2006. Research on mineral composition and Nb2O5 occurrence state of Niobium-bearing dolomite in Eastern Contact Belt of Baiyunebo Mine. Metal Mine 356, 49–52 (In Chinese with English abstract).
Zhang, Z.Q., Tang, S.H., Chen, Q.T., Wang, J.H., 1997. Sm-Nd ages and origins of metamorphic rocks for the H9 formation in the Bayan Obo ore district, and relationship with the ore forming event. Acta Geosci. Sin. 18, 267–274 (In Chinese with English abstract).
Zhang, Z.Q., Yuan, Z.X., Tang, S.H., Bai, G., and Wang, J.H., 2003. Age and geochemistry of the Bayan Obo ore deposit. Geological Publishing House, Beijing, pp. 1–222.
Zhong, Y., Zhai, M.G., Peng, P., Santosh, M., Ma, X.D., 2015. Detrital zircon U-Pb dating and whole-rock geochemistry from the clastic rocks in the northern marginal basin of the North China Craton: Constraints on depositional age and provenance of the Bayan Obo Group. Precambr. Res. 258, 133–145.
Zhu, X.K., Sun, J., Pan, C., 2015a. Sm–Nd isotopic constraints on rare-earth mineralization in the Bayan Obo ore deposit, Inner Mongolia, China. Ore Geol. Rev. 64, 543–553.
Zhu, Z.Y., Wang, R.C., Che, X.D., Zhu, J.C., Wei, X.L., Huang, X.E., 2015b. Magmatic–hydrothermal rare-element mineralization in the Songshugang granite (northeastern Jiangxi, China): Insights from an electron-microprobe study of Nb–Ta–Zr minerals. Ore Geol. Rev. 65, 749–760.